JOC The Journal of Organic Chemistry

Article

pubs.acs.org/joc

Exploitation of the Catalytic Site and 150 Cavity for Design of Influenza A Neuraminidase Inhibitors

Pal John Pal Adabala,[†] Eric B. LeGresley,[†] Nicole Bance,[‡] Masahiro Niikura,[‡] and B. Mario Pinto*,[†]

[†]Department of Chemistry and [‡]Faculty of Health Sciences, Simon Fraser University, Burnaby, British Columbia, Canada V5A 1S6

Supporting Information

ABSTRACT: We report here the exploitation of the 150 cavity in the active site of influenza A viral neuraminidases for the design of novel C-6 triazole-containing Tamiflu derivatives. A general and convenient synthetic route was developed by utilizing a highly substituted cyclic Baylis–Hillman acetate as an active precursor for azide substitution via suprafacial allylic azide [3,3]-sigmatropic rearrangement. Virus replication inhibitory assays in vitro of these triazole derivatives containing either an amino or guanidino function indicated that the guanidinium compound showed the higher efficacy against a strain with N2 subtype at a concentration of 2×10^{-5} M but did not inhibit replication of a strain with N1 subtype even at a concentration of 10^{-4} M. In order to probe the nature of the enzyme–inhibitor interactions, molecular dynamics simulations were performed on complexes of these compounds with different neuraminidase enzymes. The results indicated that the candidate inhibitors occupy both the 150 cavity and catalytic site but with alternating occupancy.

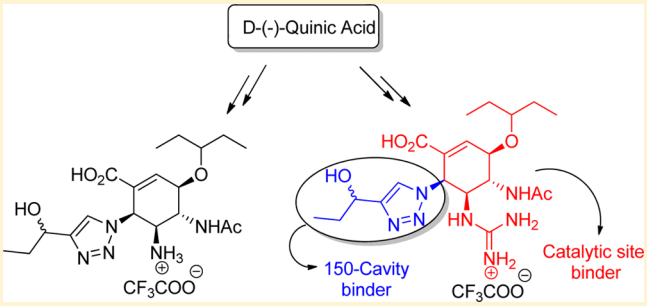

INTRODUCTION

Influenza A and B viruses can cause respiratory infections and lead to annual epidemics and infrequent pandemics.[1] Although vaccination is the primary strategy for the prevention of influenza, this approach is compromised by the necessary lead time to generate a vaccine and the requirement of annual revaccination with newly produced vaccines due to the antigenic drift. Consequently, antiviral agents play an important role in the management of influenza and are critical in preparing for a pandemic posed by an antigenically new virus to the human population such as H5N1 avian influenza A virus. Neuraminidase (NA), a surface glycoprotein of influenza virus, is a highly successful clinical target for the treatment of influenza infections.[2] Two neuraminidase inhibitors, namely Tamiflu (**1**; oseltamivir phosphate)[3] and Relenza (**2**; zanamivir),[4] are the antiviral drugs currently available to treat influenza infections (Figure 1). More recently, two other neuraminidase inhibitors, peramivir[5a] and laninamivir,[5b] were also approved as anti-influenza drugs. Despite their success, these inhibitors have limitations: for example, zanamivir suffers from low oral bioavailability, and oseltamivir is highly vulnerable to inactivation due to viral mutation.[6]

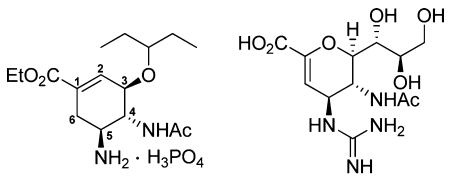

Figure 1. Anti-influenza drugs (neuraminidase inhibitors) in current use.

Influenza viral NA exists as a tetramer affixed to the viral membrane, which cleaves terminal sialic acid residues from receptors and facilitates the release of new virions from infected cells. All of the nine known neuraminidase subtypes from influenza A virus can be divided into two groups on the basis of phylogenetic analysis: group 1, consisting of N1, N4, N5, and N8 subtypes, and group 2, consisting of N2, N3, N6, N7, and N9 subtypes.[7] X-ray crystallography of several neuraminidases revealed that the active sites of groups 1 and 2 differ markedly: In group 1, a loop of amino acids, consisting of residues 147–152 (150 loop), adopts an open conformation, whereas in group 2 subtypes, this loop is closed.[8] As a result of this open-loop conformation, a cavity near the active site (150 cavity) becomes accessible to other ligands in the case of the N1, N4, N5, and N8 subtypes. The discovery of the 150 cavity has led to the development of several inhibitors designed to exploit contacts in this region and increase specificity.[9,12] However, the recent crystal structure of a partially open 150 loop in a complex of N2 with oseltamivir[10] and several in silico studies[11,12d] have indicated that movement of the 150 loop may not be restricted to group 1 NAs. Indeed, molecular dynamics (MD) studies showed that all NAs may retain the propensity for both "open" and "closed" states, maintaining an equilibrium that varies among strains.[11,12d,e]

Received: August 21, 2013
Published: October 3, 2013

In our previous studies,[12] we reported the exploitation of the 150 cavity in the active sites of group 1 neuraminidases for the design of new triazole-containing carbocycles related to oseltamivir. The most active inhibitor of the N1 enzyme[12a] (Figure 2, compound **4a**) was selective for the N1 class and

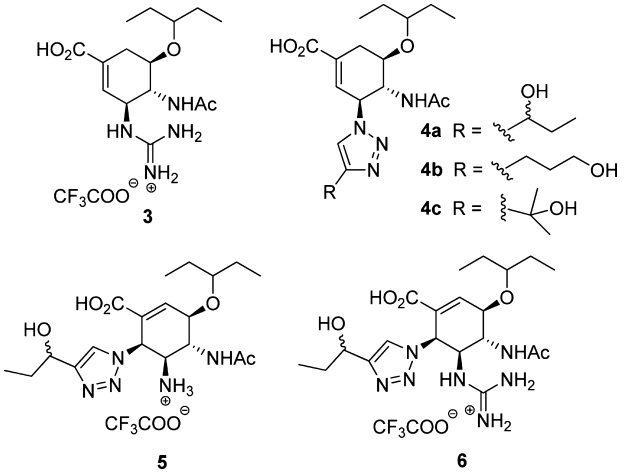

Figure 2. Previously reported neuraminidase inhibitors **3** and **4** and target compounds **5** and **6**.

showed significantly less inhibition (K_i = 2.6 vs 0.07 μM) of free influenza virus neuraminidase-2 (N2). The crystal structure of N8 complexed with these triazole-containing compounds **4a–c** (Figure 2) corroborated our design principle in which the active site and the adjoining 150 cavity are both occupied.[12e] In addition to the triazole compounds, the new candidate **3** (Figure 2) containing a guanidine function (zanamivir/oseltamivir hybrid inhibitor) was found to be a better inhibitor with a K_i value of 4.6×10^{-10} M and was active in vitro against several viral strains,[12b] including a Tamiflu-resistant (H274Y) strain.[12e] Furthermore, these compounds **3** and **4a–c** (Figure 2) did not inhibit the mammalian neuraminidases NEU3 and NEU4,[12c,e] an off-target effect observed with zanamivir.[13] Even though the 150 cavity is certainly occupied by our first-generation triazole-extended derivatives **4a–c** (Figure 2), these compounds were still not active enough in the virus replication inhibition assay to warrant further development.[12b] This is likely because of the absence of hydrogen-bonding interactions between the amino or guanidino function with the catalytic site amino acids Asp151 and Glu 119 to anchor the compounds. These results are corroborated by MD studies in which the triazole group (TG) is not stable in the 150 cavity but exits the subsite periodically.[12d,e] To re-establish the hydrogen-bonding network of basic groups with Asp151 and Glu 119, we designed the next-generation compounds **5** and **6** (Figure 2), which contain the amino or guanidine group as well as the TG to occupy both the catalytic site and the 150 cavity. The rationale behind this approach is that the C-6 methylene carbon of oseltamivir is also oriented toward the 150 cavity[8a] and, hence, shifting the substituted triazole group to this position would also give access to the 150 cavity. Another consequence of this approach is that the position of the double bond in the new series will be same as in that in oseltamivir, as opposed to our first generation of compounds. We believe, as before,[12] that targeting both subsites with these next-generation dual-site inhibitors will lead to reduced potential for development of resistance and such inhibitors could lead to new anti-influenza drugs that would add to the current arsenal. Most of the previous work related to 150 cavity binders was developed on the basis of the zanamivir skeleton.[9] We report here the synthesis of the next-generation carbocyclic candidates, their evaluation in vitro against viral strains, and their molecular dynamics (MD) studies in complexes with different neuraminidase enzymes. To attain the target molecules, we have chosen our previously reported[12a] intermediate **7** (Scheme 1) as the starting material.

RESULTS AND DISCUSSION

Synthesis. As depicted in Scheme 1, we have synthesized the target molecules by functionalizing the C-1, C-2, and C-6 positions of the chiral azide **7** by using dihydroxylation, sulfuryl chloride mediated elimination, and azidation of the allylic acetate via allylic azide [3,3]-sigmatropic rearrangement as the key reactions. Initial attempts with osmium tetroxide mediated dihydroxylation of unsaturated ester **7** under various experimental conditions failed. To overcome the unreactive nature of olefin **7** toward the dihydroxylation, we chose a mild and highly reactive ruthenium-based bimetallic oxidizing system[14] ($RuCl_3$/$CeCl_3 \cdot 7H_2O$/$NaIO_4$) for its dihydroxylation. Thus, treatment of unsaturated ester **7** with a catalytic amount of $RuCl_3$ in the presence of $CeCl_3$/$NaIO_4$ in a mixed solvent system (EtOAc/

Scheme 1. Synthesis of the Key Intermediate 12

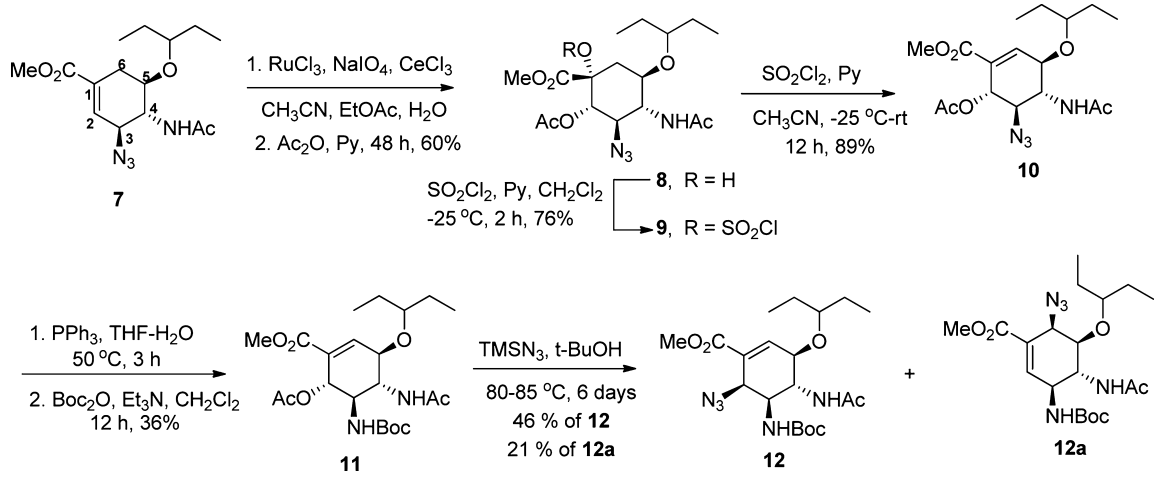

dx.doi.org/10.1021/jo401854w | J. Org. Chem. 2013, 78, 10867–10877

CH_3CN/H_2O, 3/3/1) at 0 °C provided an α-diol with high diastereoselectivity. Acetylation of the resulting diol in the presence of Ac_2O/Py gave the monoacetate **8** in 60% overall yield. The configurations at C-1 and C-2 were confirmed by NMR spectroscopy. The large coupling constants (i.e., >10.0 Hz) for $J_{2,3}$, $J_{3,4}$, and $J_{4,5}$ and cross-peaks between H-2, H-4, and H-6b in the $^1H-^1H$ NOESY spectrum of compound **8** clearly showed the existence of the chair conformation (Figure 3) and the formation of the α-diol in the dihydroxylation reaction.

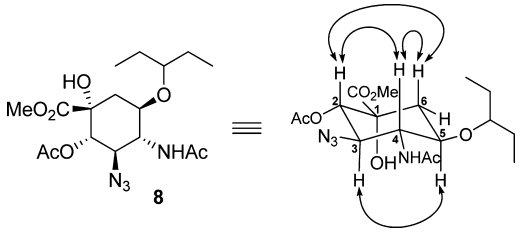

Figure 3. Observed $^1H-^1H$ NOESY contacts for compound **8**.

Eliminations of the alcohol function in **8** with various reagents such as Martin sulfurane,[15] Burgess reagent,[16] Vilsmeier reagent,[17] and other classical methods ($POCl_3$, $SOCl_2$, OTf elimination)[18] were unsuccessful or were very low yielding. The elimination reaction was finally achieved with sulfuryl chloride. Initial experiments with SO_2Cl_2 in the presence of pyridine in CH_2Cl_2 furnished the chlorosulfate **9** as the only product, which was used for the preparation of olefin **10** using basic conditions or by heating. Subsequently, the elimination reaction was accomplished in excellent yields in a one-step process using CH_3CN as solvent with SO_2Cl_2 in the presence of pyridine. Owing to the residual sulfur products in olefin **10**, the reduction of the azide using Lindlar catalyst with H_2 (1 atm) was unsuccessful. However, reduction of the azide **10** with PPh_3 in $THF-H_2O$ at 50 °C provided the corresponding free amine, which on treatment with *tert*-butylpyrocarbonate afforded the Boc-protected amine **11** (Scheme 1).

Initially, we prepared the related mesylate derivative instead of the acetate **11** for the nucleophilic substitution reactions. However, the mesylate was highly unstable and compromised further reactions. Therefore, the crucial nucleophilic substitution was examined using the allylic acetate **11** (Scheme 1), a cyclic Baylis–Hillman derivative. Initial attempts at substitution reactions with sodium azide in different polar solvents led to a complex mixture of products. Finally, the desired azide **12** was obtained in 46% yield by treatment of **11** with $TMSN_3$ in t-BuOH, a side product **12a** also being formed. Controlling the regioselectivity of this reaction under various reaction conditions proved to be difficult and depended on the neighboring substituents and nature of the leaving groups.

The stereochemistry of the azide **12** was confirmed by NMR spectroscopic analysis. The ^1H NMR spectrum of compound **12** showed small vicinal coupling constants (<4.0 Hz) for $J_{3,4}$, $J_{4,5}$, and $J_{5,6}$, which contrast with the coupling constants observed in the acetate **11**. In the latter case, the large coupling constants for $J_{3,4}$, $J_{4,5}$, and $J_{5,6}$ (>6.5 Hz) clearly confirmed the preponderance of the preferred half-chair conformation **11-I** (Figure 4). The lower coupling constants in azide **12** would be consistent with an albeit unlikely half-chair conformation in which the bulky groups occupy axial or pseudoaxial positions. However, NOE contacts between H-6/H-5 and H-6/NHBoc and examination of molecular models suggested that **12** more likely exists in the boatlike conformation **12-I** (H-6 *gauche* to H-5 and −NHBoc, Figure 4), in which the dihedral angles between H-3/H-4, H-4/H-5, and H-5/H-6 correlate with their coupling constants. If the desired azide **12** were an α-azide (**12b**; Figure 4), it would be unlikely to exist in the half-chair conformation **12b-I** (Figure 4), in which all the bulky groups occupy axial or pseudoaxial positions, resulting in small coupling constants. This would also contrast with the conformation of the α-acetate **11**, in which all the bulky groups occupy equatorial positions, resulting in large coupling constants. Furthermore, a boatlike conformation of the α-azide

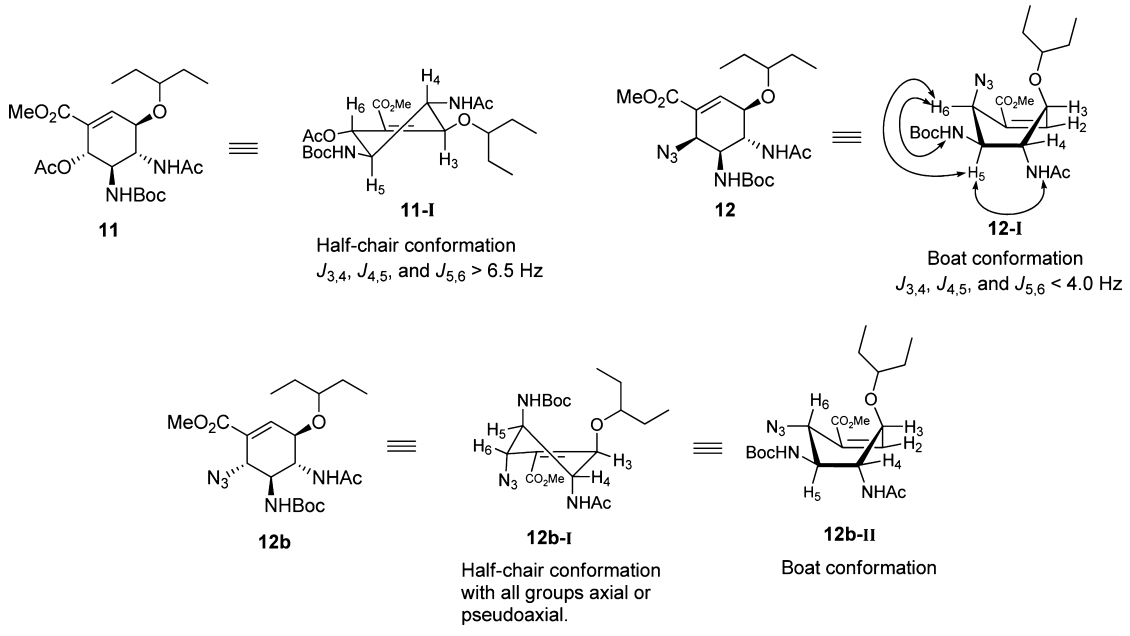

Figure 4. Conformational analysis of **11**, **12**, and **12b**. Double-headed arrows indicate NOE contacts.

dx.doi.org/10.1021/jo401854w | J. Org. Chem. 2013, 78, 10867−10877

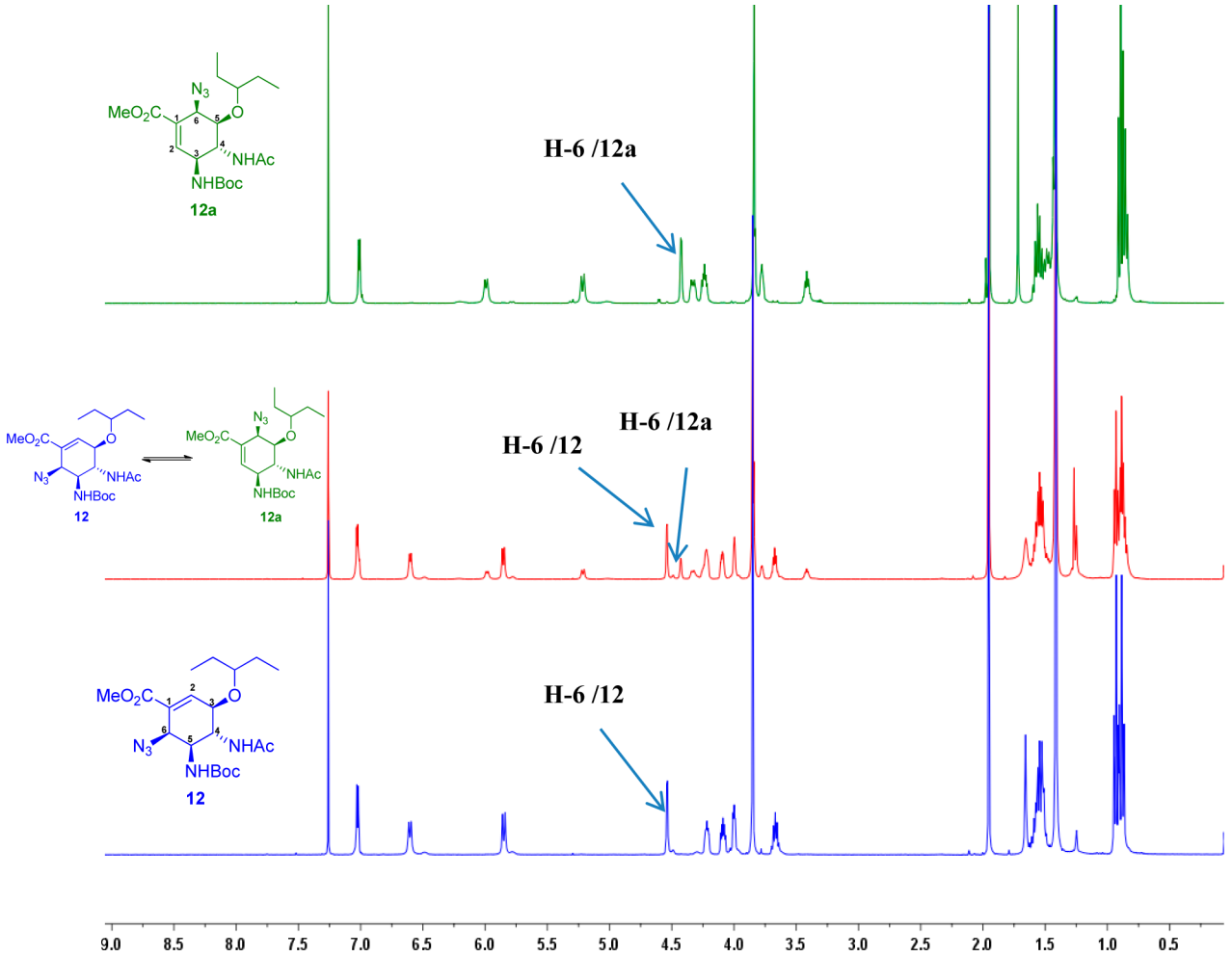

Figure 5. ^{1}H NMR spectra of **12** (bottom trace), **12a** (top trace), and the mixture (center trace) obtained by equilibration of either isomer.

12b (**12b-II**; Figure 4) would not be consistent with the small coupling constant for $J_{5,6}$ and the observed NOE correlations. Therefore, the collective evidence suggests that **12** is in fact the β-azide.

The desired azide **12** could have arisen from S_N2 substitution of the acetate by the azide nucleophile, or alternatively, via allylic azide [3,3]-sigmatropic rearrangement. Such thermally facile rearrangements have precedent in the literature.[19] Indeed, heating either isomer **12** or **12a** in t-BuOH at reflux led to the formation of an equilibrium mixture of **12** and **12a** in a 2.2:1 ratio (Figure 5), where the individual regioisomers are stable at room temperature for longer durations. The azide **12a** is thus the kinetic product, which rearranges to give an equilibrium mixture of **12** (thermodynamic product) and **12a**. The allylic azide **12a** likely results from the conjugate addition of the azide nucleophile on the unsaturated ester, which forms a stabilized anion, followed by the E1cB elimination of the acetate. The azide substituent in **12a** was also assigned to the β orientation because thermally allowed [3,3]-sigmatropic rearrangements proceed in a suprafacial manner.[19] This configuration was also confirmed by NMR spectroscopy. The small coupling constants for $J_{3,4}$, $J_{4,5}$, and $J_{5,6}$ (<4.8 Hz), the observed NOE correlations between H-6/H-5 and H-6/H′ (hydrogen from the isopentyloxy group), and an examination of molecular models suggested that the azide **12a** also exists in the boatlike conformation **12a-I** (Figure 6).

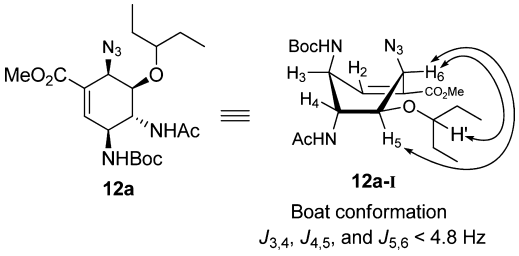

Figure 6. Conformational analysis of **12a**. Double-headed arrows indicate NOE contacts.

Having the desired azide **12** in hand, we next turned our attention to the target molecules **5** and **6**. The copper-catalyzed azide−alkyne cycloaddition reaction[12a,20] with azide **12** and 1-pentyn-3-ol using the standard protocol provided the triazole **13** in 71% yield. Hydrolysis of the methyl ester **13** was performed using 1 M KOH in THF. The desired carboxylic acid **14** was precipitated by the addition of EtOAc to the column-purified acid. The NHBoc deprotection of acid **14** with TFA furnished the target compound **5** in 88% yield (Scheme 2).

The triazole **13** was next used for the synthesis of guanidinium derivatives **17** and **6**. Thus, the Boc deprotection of carbamate **13** under acidic conditions followed by treatment with basic Amberlyst A26 resin gave the free amine, which was then converted into the Boc-protected guanidine derivative **16**

dx.doi.org/10.1021/jo401854w | J. Org. Chem. 2013, 78, 10867−10877

Scheme 2. Synthesis of Target Compound 5

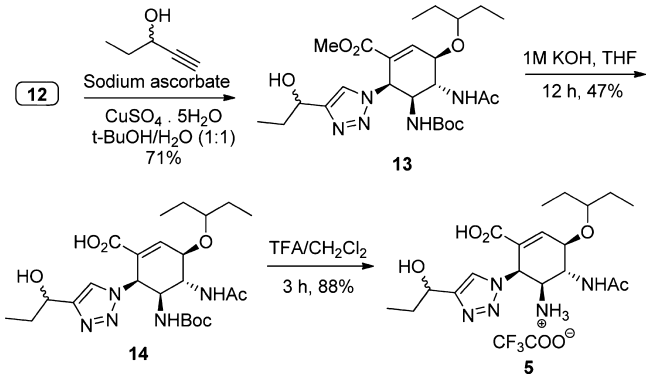

using Boc-protected thiourea and $HgCl_2$, and the Boc groups were removed to give **17**, as shown in Scheme 3. However,

Scheme 3. Synthesis of Target Compound 6

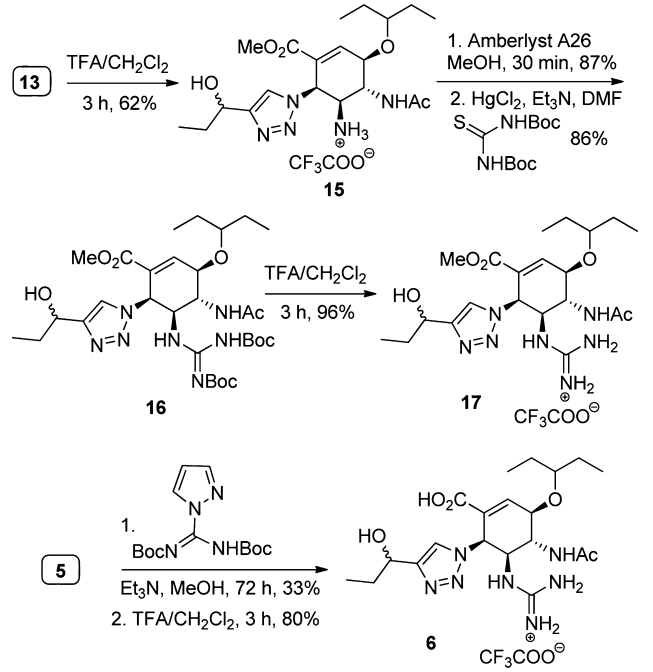

hydrolysis of the methyl esters **16** and **17** into their respective acids was problematic even with mild Me_3SnOH hydrolysis. The target guanidinium salt **6** was obtained finally in modest yield from **5** by introduction of the Boc-protected guanidine group using Boc-protected 1*H*-pyrazole-1-carboxamidine and subsequent Boc deprotection with TFA (Scheme 3).

In this synthesis we have used racemic 1-pentyl-3-ol and synthesized compounds **5** and **6** as diastereomeric mixtures. In our previous report,[12a] compound **4a** (Figure 2) as a diastereomeric mixture was the most active 150 cavity binder. In a recent publication,[12e] we have reported the crystal structures of each of these isomers (**4a**, Figure 2) in complexes with the neuraminidase enzyme N8. Both compounds bind in similar modes and are both presumably active. On the basis of these results, our initial investigation of compounds **5** and **6** as 150 cavity binders also dealt with diastereomeric mixtures. Future work will involve examination of individual diastereomers.

Cell Culture Assays. In our previous work[12a] we reported in vitro enzyme inhibition assays. However, we have found that even compounds showing nanomolar inhibition of the pure enzymes were not active when tested in cell culture assays.[12b] The latter tests are therefore a more robust, albeit humbling, test for whether active compounds, which could be developed further as drug candidates, are present. In general, one loses 3–4 orders of magnitude in activity on going from in vitro enzyme assays to cell-based assays. Therefore, in order to investigate the efficacy of the compounds against influenza A virus, the three compounds **5**, **6**, and **17** were tested in an in vitro replication inhibition assay using A/Puerto Rico/8/34 (PR8, H1N1) and A/Hong Kong/1/68 (HK1, H3N2) strains.[12b] As shown in Table 1, compound **6** showed the highest efficacy against the

Table 1. Inhibitory Effects of the Compounds against PR8 (H1N1) and HK1 (H3N2) Strains[a]

	5		6		17	
concn (M)	PR8	HK1	PR8	HK1	PR8	HK1
1×10^{-4}	−	+	−	+	−	+
2×10^{-5}	−	±	−	+	−	±
4×10^{-6}	−	−	−	±	−	−

[a]Test monolayers were infected at 50TCID50. All experiments were performed along with a back-titration in which 50TCID50 always resulted in clear infection (i.e., results similar to no inhibition) in all wells. Legend: +, inhibition; ±, incomplete inhibition; −, no inhibition.

HK1 strain at a concentration of 2×10^{-5} M. The methyl ester **17**, which contains the free guanidine group, and the amino acid **5** also showed inhibitory effects at 1×10^{-4} M against the HK1 strain. However, the inhibitory effect of these compounds was limited to the HK1 strain and they did not inhibit replication of the N1 subtype (PR8) even at a concentration of 10^{-4} M. The inhibitory effects of these compounds were significantly increased in comparison to our first-generation triazole compounds.[12b]

Molecular Dynamics Studies. The MD simulations of the *R* and *S* diastereomers of compounds **5** and **6** were examined. They behaved similarly, and so only the simulations of the *R* isomer are described (Figure 7). The subtle differences in binding between diastereomers do not appear to be significant, and this portion of the molecule is ejected from the 150 subsite during the simulations. Thus, MD simulations were performed on compounds **5** and **6** in complexes with four monomers (T2, $T1_2$, $T1_{open}$, and $T1_{closed}$) of influenza neuraminidase (see the Experimental Section and Supporting Information for details); the reported crystal structures had either open or closed 150 loops. The behaviors of the *R* and *S* stereoisomers at the propyloxy function were similar. Compounds **5** and **6** were docked onto each of T2, $T1_2$, $T1_{open}$, and $T1_{closed}$ using Autodock Vina[21] before three independent molecular dynamics trajectories were collected using standard parameters,[12d] for each combination, as noted above. Using combined clustering with conserved active site residues[12d] as well as residues 147–152 (the 150 loop), significant conformations of compounds **5** and **6** and important conformations of the enzymes were determined and the data were compared.

In every dynamics simulation except for the $N1_{closed}$-**6** complex, the inhibitor stayed bound in the active site of its respective enzyme. However, retaining oseltamivir-like interactions while gaining interactions in the 150 cavity via the triazole-linked group (TG) was compromised. In the T2-**5**

dx.doi.org/10.1021/jo401854w | J. Org. Chem. 2013, 78, 10867–10877

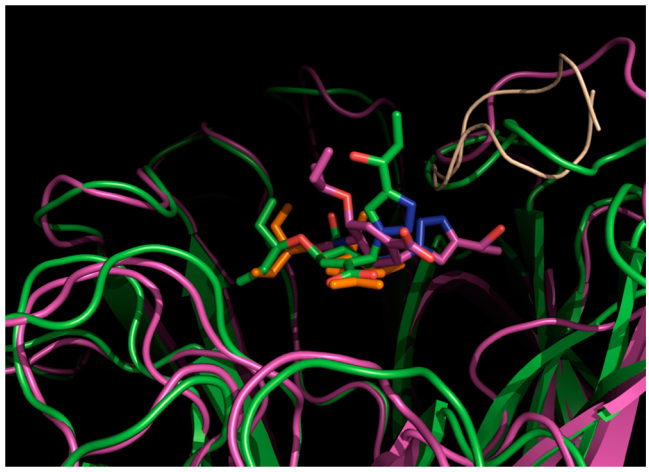

Figure 7. Poses from MD simulations: The beige ribbons represent the open and closed conformations of the 150 loop from the crystal structures of $T1_{open}$ and $T1_{closed}$, respectively. The magenta enzyme cartoon represents a hyper-open-loop structure from dynamics simulations. The green enzyme cartoon represents a closed-loop structure from dynamics simulations. The crystal structure position of oseltamivir in $T1_{open}$ and $T1_{closed}$ is shown by orange sticks. The extremes of the "see-saw" motion are shown as green and magenta sticks. The green sticks show the oseltamivir-like pose, and the magenta sticks show a pose where the TG is bound in the 150 cavity. Note the relative positions of the central rings.

complex, the ligand consistently translated away from the 150 cavity and tilted such that the TG became trapped underneath Asp151 of the 150 loop. Although at any one time one or two of the amino, carboxyl, or pentyloxy groups interacted with the enzyme, no sustained interactions occurred. The amide group lost all contacts, but the hydroxyl group of the TG maintained hydrogen bonding with Asp151 or Glu119 throughout all three of the triplicate runs. The enzyme interconverted between closed and open states. In the T2-**6** complex, the triazole ring of the ligand was pushed away from the 150 cavity and retained a vertical conformation with respect to the enzyme active site, the TG was buried in the enzyme adjacent to the 150 cavity, and the 150 loop retained a fully closed conformation. In the $T1_2$-**5** complex, the ligand exhibited oseltamivir-like interactions, although the TG was ejected into solution, and because of slight translation away from the 150 cavity, the pentyloxy group lost many interactions due to steric clashes. The 150 loop, although primarily closed, occasionally adopted an open conformation. When compound **6** was complexed to $T1_2$, the ligand adopted two main conformations: the first was similar to oseltamivir, although like the $T1_2$-**5** complex, the TG and the pentyloxy group exited the subsites. The second consisted of the TG buried in the enzyme next to the 150 cavity, and all oseltamivir-like interactions were lost except for the guanidine group, which interacts with Glu277 and Glu119. The 150 loop oscillated between the open and closed conformations. In the $T1_{open}$-**5** complex, the ligand either adopted an oseltamivir-like conformation with the TG in solution (minor conformation) or a conformation in which all oseltamivir-like interactions were lost except for the amino group, which interacted with Glu119, and the TG, which was pulled under Arg151 where its OH group interacted with Arg151. The 150 loop maintained a hyper-open conformation. When compound **6** was complexed with $N1_{open}$, it maintained oseltamivir-like interactions but was translated 1.5 Å away from the 150 cavity relative to oseltamivir. The TG and the pentyloxy groups were exposed to solution. The 150 loop again adopted an overly open position. The $T1_{closed}$-**5** complex resulted in the ligand moving between an oseltamivir-like state with the pentyloxy group and the TG in solution and a conformation in which the TG entered the 150 cavity or slid under Asp151 but with all oseltamivir-like interactions lost, except for the amino−Glu119 interaction. The 150 loop moved to an open or very open position. In the $T1_{closed}$-**6** simulations, the ligand exited the active site and the 150 loop oscillated from a closed to an open conformation.

The fluctuations of the enzymes were as follows: T2 < $T1_2$ < $T1_{open}$ = $T1_{closed}$. As the dynamics of the subtype increased, both **5** and **6** appeared to be less strained and tended to prefer an oseltamivir-like pose where the TG was in solution over a conformation where the TG was bound to the enzyme and most oseltamivir-like interactions were lost. In the more dynamic enzymes, the guanidine moiety consistently made better contacts with proximal acidic residues than the amino group due to its larger size. The translation of the triazole ring away from the 150 cavity when either ligand was in an oseltamivir-like conformation is attributable to steric clashes between the TG and residues in the 150 loop. These steric clashes were present in virtually all conformations and were relieved by loop opening. In summary, compounds **5** and **6** can either maintain contacts in the active site but suffer ejection of the TG into solution or severely compromise contacts in the active site so that the TG can bind to the 150 cavity. This "see-saw" effect is caused by the large (~60°) angle between the central ring and the TG and the fact that the TG is too short to allow simultaneous occupation of both 150 cavity and the catalytic site.

CONCLUSIONS

In conclusion, we have successfully synthesized C-6 triazole-functionalized Tamiflu derivatives as second-generation candidates using an azidation reaction on the cyclic Baylis−Hillman derivative **11** via allylic azide [3,3]-sigmatropic rearrangement and copper-catalyzed azide−alkyne cycloaddition as key reactions. These new candidates were designed to target both the catalytic site and the 150 cavity of influenza virus NA. The guanidinium compound **6** showed promising inhibitory activity against HK1 (H3N2) strain at a concentration of 2×10^{-5} M and also showed activity against PR8 (H1N1) strain but at higher concentrations ($>1 \times 10^{-4}$ M). Although the 150 cavity is certainly occupied by these molecules, molecular dynamics simulations suggest that further optimization will be required at the C-6 position in order to sustain interactions with both the catalytic site and the 150 cavity. These results provide further insight into the requirements of an effective inhibitor of influenza neuraminidase through multisubsite occupation.

EXPERIMENTAL SECTION

General Methods. ^1H and ^{13}C NMR spectra were recorded at 600 or 400 MHz and 150 or 100 MHz, respectively. All assignments were confirmed with the aid of two-dimensional $^1H-^1H$ (COSY) and/or $^1H-^{13}C$ (HSQC) experiments using standard pulse programs. Processing of the spectra was performed with MestReNova software. Analytical thin-layer chromatography (TLC) was performed on aluminum plates precoated with silica gel 60F-254 as the adsorbent. The developed plates were air dried, exposed to UV light, and/or sprayed with a solution containing 1% $Ce(SO_4)_2$ and 1.5% molybdic acid in 10% aqueous H_2SO_4, and heated. Column chromatography was performed with an automated flash chromatography system. High-

dx.doi.org/10.1021/jo401854w | J. Org. Chem. 2013, 78, 10867−10877

resolution mass spectra were obtained by the electrospray ionization method, using a TOF LC/MS high-resolution magnetic sector mass spectrometer.

Virus Inhibition Assay. *Cells and Viruses.* Influenza A virus strains A/Puerto Rico/8/32 (PR8, H1N1) and A/Hong Kong/1/68 (HK1, H3N2), both of which are mouse-adapted, were obtained from Dr. E. Brown (University of Ottawa). MDCK cells were maintained in DMEM supplemented with 10% FBS and antibiotics. After the infection the monolayers were maintained in DMEM with 0.00075% trypsin (Difco) and antibiotics without FBS (DMEM-trypsin).

$TCID_{50}$. Tissue culture infectious dose 50 ($TCID_{50}$) values of the IFV stocks were determined by inoculating 100 μL of diluted virus stocks in DMEM−trypsin to the MDCK monolayers in 96-well plates. In the case of the HK1 strain, the infection of IFV was visually determined by the cytopathic effect (CPE) under a light microscope on 2 and 3 days of infection. For determination of the infection of strain PR8, which does not produce specific CPE on an MDCK monolayer, the infected monolayers were fixed by methanol−acetone (1/1) and immunostained by PR8-specific chicken antiserum (Charles River) and FITC-labeled antichicken IgY (Sigma) after 2 days of infection. The monolayers that showed the lack of spread of positive staining rather than the lack of individual cell staining were considered as infection positive. $TCID_{50}$ was calculated by the Reed and Müench method from the results of eight wells for each dilution.

Inhibition Test. To test the replication inhibition efficacy, the compounds were dissolved in methanol and then diluted at least 100 times in DMEM−trypsin.[12b] A fifty microliter portion of each diluted test compound was added to each well of MDCK monolayers in 96 wells and then followed by 50 μL of virus suspension (50 $TCID_{50}$) prepared DMEM−trypsin. The test was performed in quadruplicate. The inhibition effect was regarded positive when the virus spread was not observed by the same criteria as used for the determination of $TCID_{50}$.

Computational Studies. *Preparation of Enzyme Monomers.* Four monomers of neuraminidase were used in this study: a typical type 2 neuraminidase from A/Memphis/31/1998(H3N2) with a traditionally closed 150 loop (PDB code 2AEP; referred to as T2), a type 1 neuraminidase from A/California/04/2009(H1N1) prone to loop closure[22] (PDB code 3NSS; referred to as $T1_2$), and a typical type 1 neuraminidase from A/duck/Ukraine/01/1963(H3N8) crystallized in both 150 loop open and closed conformations (PDB codes 2HT7 and 2HT8, respectively; referred to as $T1_{open}$ and $T2_{closed}$, respectively). In preparation for molecular dynamics, the enzyme PDBs were modified. All PDB structures were first passed to MolProbity,[23] where their structure was ensured to be free of error and corrected if necessary. If the PDB structure had more than one monomer, the monomer with the least errors was chosen to carry on. The monomers were then passed to the PDB2PQR server,[24] where all amino acids were protonated on the basis of a pH of 6.5. The coordinates were retrieved, and the monomers were aligned. All non amino acid atoms were removed, and disulfide bridges were created and verified. Also, the Ca^{2+} ion proximal to the binding site was added if missing,[25] and nonclashing crystal structure bound water was readded to each monomer. The enzyme files were renumbered and saved as AMBER files using the tleap tool in Amber 12.0.[26]

Ligand Preparation. The ligand parametrization consisted of two main steps: partial charge derivation (RESP)[27] and atom-type assignment. Because small perturbations in molecular structure were found to make vast differences in charge distribution over the ligand, eight independent quantum mechanical optimizations were performed at the Hartree−Fock level with the 6-31G* basis set in Gaussian09,[28] giving eight minimized structures per compound, from which charges were derived. The partial charges were computed by the R.E.D. server[29] using single-point electrostatics calculations in multiple orientations. The final charge set for each molecule was selected on the basis of consistency with the Amber ff99SB force field[30] parameters and previous partial charge calculations.[12d] All generalized amber force field[31] (GAFF) atom types for the compounds were assigned automatically by antechamber and checked manually for errors. As with the enzyme, AMBER files for the ligands were finalized by tleap.

Docking. Before molecular dynamics simulations, the compounds were docked onto the enzymes using AutoDock Vina.[21] Initial poses for molecular dynamics were chosen on the basis of conformation rank and similarity to binding poses of existing inhibitors. Both *R* and *S* isomers about the propyloxy function were examined.

Molecular Dynamics Simulations. MD simulations of all systems were conducted with the GROMACS suite, version 4.6,[32] utilizing the Amber ff99SB force field. AMBER files for each complex were converted into GROMACS formats using ACPYPE[33] with the "gmx45" option. Each system was placed in a dodecahedral box with a minimal 12 Å distance between solute and box edge and solvated with TIP3P water molecules. Salt ions were then introduced to achieve a concentration of 0.15 M and neutralize the overall charge. Each system was then treated to at least two alternating rounds of 5000 steps each steepest descent and conjugate gradient minimization. Following minimization, random velocities were generated in the first step of equilibration to yield unique triplicate runs of each system. Equilibration entailed first gradually heating the system from 0 to 300 K in 60 K increments with a Berendsen thermostat during simulations of 40 ps duration. Position restraints on solute molecules began at 1000 kJ mol^{-1} nm^{-2} and were reduced by 200 kJ mol^{-1} nm^{-2} per incremental run. The pressure was then equilibrated during three steps, first, with 200 kJ mol^{-1} nm^{-2} solute restraints, a Berendsen barostat with a time constant of 2.0 ps and a reference pressure of 1.0 atm, and a Berendsen thermostat with a time constant of 0.5 ps and a reference temperature of 298 K. After 100 ps, position restraints were removed for an additional 100 ps simulation. Finally, the pressure and heat controls were changed to a Nose−Hoover[34] thermostat and a Parrinello−Raham barostat,[35] and the system was equilibrated for a final 400 ps before beginning production runs with the same configuration. Throughout, the LINCS algorithm was used to constrain bonds involving hydrogen atoms and the leapfrog integrator was employed with a 2 fs time step. Short-range interactions were calculated with a cutoff of 1.0 nm for Columbic interactions and 1.3 nm for van der Waals interactions. Long-range electrostatic interactions were calculated with the particle mesh Ewald (PME) algorithm using a grid spacing of 0.12 nm and an interpolation order of 4. Neighbor lists with a 1.0 nm cutoff were updated every five steps.

Combined Clustering and General Analysis. Previous results[12d] have shown that achievement of backbone stability in similar situations takes no longer than 20 ns. Therefore, the first 20 ns of each triplicate run was discarded as "extra equilibration" before combined clustering analysis.[12d] Combined clustering was performed by extracting the concatenated enzyme trajectories from all systems. Both trajectories of the same enzyme were then concatenated. An RMSD matrix for the combined trajectories of each was then calculated from a time step of 50 ps and based on the side chain heavy atoms of key, conserved active site residues (R118, E119, W178, R224, E227, E276, E277, R292, R371, Y406) and the mobile 150 loop residues (147−152). Clustering was then performed on each combined enzyme trajectory using the GROMOS algorithm,[36] as implemented in the GROMACS package with an RMSD cutoff of 0.16 nm between each cluster. This cutoff was chosen as the optimal balance between the number of clusters and their meaningfulness. Ligands were clustered separately by the same method, although on the basis of all heavy atoms of the compound and an RMSD cutoff of 0.15 nm. Results for the enzymes were separated and sorted via custom Bash Shell scripts and assembled along with the ligand clusters in spreadsheets to facilitate interpretation. The results of the combined clustering are detailed in the Supporting Information (SI 1 and 2). RMSD values of the heavy atoms of the enzyme backbones were computed to confirm enzyme stability (Supporting Information, SI 3). Center of mass (COM) distances from the heavy atoms of the enzymes to the heavy atoms of the ligands were also measured (Supporting Information, SI 4). Both the backbone RMSD and the COM distance measurements were done on the full 100 ns runs.

Methyl (1*R*,2*S*,3*R*,4*R*,5*R*)-4-Acetamido-2-acetoxy-3-azido-5-(1-ethylpropoxy)-1-hydroxycyclohexane-1-carboxylate (8). A mixture of $NaIO_4$ (990.1 mg, 4.621 mmol) and $CeCl_3{\cdot}7H_2O$ (76.2 mg, 0.309 mmol) in H_2O (6.0 mL) was stirred at room temperature for a

dx.doi.org/10.1021/jo401854w | J. Org. Chem. 2013, 78, 10867−10877

few minutes. The reaction mixture was cooled to 0 °C, and EtOAc (9.0 mL), CH_3CN (18.0 mL), and $RuCl_3·H_2O$ (16.0 mg, 0.077 mmol) were added successively. After the mixture was stirred for 2.0 min, a solution of olefin **7** (1.0 g, 3.086 mmol) in EtOAc (9.0 mL) was added, and the resulting heterogeneous mixture was stirred until the reaction was complete (TLC monitoring). The reaction mixture was diluted with EtOAc (300 mL). The organic layer was washed with aqueous $NaHCO_3$ and water, dried (Na_2SO_4), and concentrated under reduced pressure. The crude diol (860 mg, 2.401 mmol) was dissolved in pyridine (10.0 mL) and acetic anhydride (0.7 mL, 7.203 mmol), and the resulting reaction mixture was stirred at room temperature for 2 days. The reaction mixture was diluted with ethyl acetate (300 mL) and washed with water (300 mL). The organic layer was washed with 2 M H_2SO_4 and aqueous $NaHCO_3$, dried over anhydrous Na_2SO_4, and concentrated under reduced pressure. The crude product was purified using flash chromatography (hexanes/EtOAc 1/1) to give monoacetate **8** as a white solid (740 mg, 60% yield for two steps). $[\alpha]_D^{23}$ = −35.24° (*c* 1.05, CH_2Cl_2). ^{1}H NMR (400 MHz, $CDCl_3$): δ 6.36 (d, $J_{4,NH}$ = 8.2 Hz, 1H, −N*H*), 5.04 (d, $J_{2,3}$ = 10.2 Hz, 1H, H-2), 4.35 (t, $J_{2,3} = J_{3,4}$ = 10.6 Hz, 1H, H-3), 3.94 (td, $J_{4,5} = J_{5,6b}$ = 10.9, $J_{5,6a}$ = 4.6 Hz, 1H, H-5), 3.74 (s, 3H, −COOC*H*$_3$), 3.63 (d, $J_{1,OH}$ = 1.5 Hz, 1H, 1-O*H*), 3.50 (dt, $J_{3,4} = J_{4,5}$ = 10.4, $J_{4,NH}$ = 8.5 Hz, 1H, H-4), 3.17 (p, *J* = 5.6 Hz, 1H, −OC*H*(CH$_2$CH$_3$)$_2$), 2.18−2.08 (m, 1H, H-6a), 2.13 (s, 3H, −OCOC*H*$_3$), 2.03 (s, 3H, −NHCOC*H*$_3$), 1.90−1.84 (m, 1H, H-6b), 1.52−1.33 (m, 4H, −OCH(C*H*$_2$CH$_3$)$_2$), 0.85 and 0.83 (t, *J* = 7.3 Hz, 3H, −OCH(CH$_2$C*H*$_3$)$_2$). ^{13}C NMR (100 MHz, $CDCl_3$): δ 173.1 (−COOCH$_3$), 170.7 (−NHCOCH$_3$), 169.3 (−OCOCH$_3$), 81.5 (−OCH(CH$_2$CH$_3$)$_2$), 75.2 (C-2), 74.7 (C-1), 71.4 (C-5), 61.4 (C-3), 57.8 (C-4), 53.5 (−COOCH$_3$), 36.9 (C-6), 26.0 and 25.8 (−OCH(CH$_2$CH$_3$)$_2$), 23.5 (−NHCOCH$_3$), 20.5 (−OCOCH$_3$), 9.7 and 9.1 (−OCH(CH$_2$CH$_3$)$_2$). HRMS: *m*/*z* calcd for $C_{17}H_{28}N_4O_7Na$ [M + Na]$^+$ 423.1850, found 423.1854.

Methyl (1*R*,2*S*,3*R*,4*R*,5*R*)-4-Acetamido-2-acetoxy-3-azido-1-((chlorosulfonyl)oxy)-5-(1-ethylpropoxy)cyclohexane-1-carboxylate (9). A solution of alcohol **8** (150 mg, 0.374 mmol) and pyridine (0.18 mL, 2.244 mmol) in CH_2Cl_2 (36.0 mL) was cooled to −25 °C and added dropwise to sulfuryl chloride (0.045 mL, 0.561 mmol) over 5 min. The reaction mixture was stirred at this temperature for 2 h, and excess sulfuryl chloride was decomposed by dropwise addition of EtOH (0.04 mL). The mixture was warmed to 0−5 °C and washed with 2 M sulfuric acid (50 mL). The aqueous layer was back-extracted with CH_2Cl_2 (50 mL), and the organic layers were combined and washed with water, followed by 5% aqueous $NaHCO_3$, and dried over anhydrous Na_2SO_4. Evaporation of the solvent gave the crude product, which was purified by flash column chromatography (hexanes/EtOAc 7/3) to give compound **9** as a colorless liquid (143.0 mg, 76% yield). $[\alpha]_D^{23}$ = −42.73° (*c* 1.1, CH_2Cl_2). ^{1}H NMR (400 MHz, $CDCl_3$): δ 5.87 (d, $J_{4,NH}$ = 6.8 Hz, 1H, −N*H*Ac), 5.08 (d, $J_{2,3}$ = 10.3 Hz, 1H, H-2), 4.58 (t, $J_{2,3} = J_{3,4}$ = 10.7 Hz, 1H, H-3), 4.30 (td, $J_{4,5} = J_{5,6b}$ = 11.2, $J_{5,6a}$ = 4.3 Hz, 1H, H-5), 3.79 (s, 3H, −COOC*H*$_3$), 3.27−3.16 (m, 2H, H-4, −OC*H*(CH$_2$CH$_3$)$_2$), 3.00 (dd, $J_{6a,6b}$ = 15.6, $J_{5,6a}$ = 4.3 Hz, 1H, H-6a), 2.14 (s, 3H, −OCOC*H*$_3$), 2.10 (dd, $J_{6a,6b}$ = 15.6, $J_{5,6b}$ = 11.5 Hz, 1H, H-6b), 2.04 (s, 3H, −NHCOC*H*$_3$), 1.52−1.38 (m, 4H, −OCH(C*H*$_2$CH$_3$)$_2$), 0.86 and 0.85 (t, *J* = 7.4 Hz, 3H, OCH(CH$_2$C*H*$_3$)$_2$). ^{13}C NMR (150 MHz, $CDCl_3$): δ 170.9 (−NHCOCH$_3$), 169.4 (−OCOCH$_3$), 165.7 (−COOCH$_3$), 93.3 (C-1), 81.7 (−OCH(CH$_2$CH$_3$)$_2$), 73.4 (C-2), 69.7 (C-5), 60.0 (C-3), 58.5 (C-4), 54.1 (−COOCH$_3$), 34.9 (C-6), 26.0 and 25.7 (−OCH(CH$_2$CH$_3$)$_2$), 23.8 (−NHCOCH$_3$), 20.4 (−OCOCH$_3$), 9.6 and 9.2 (−OCH(CH$_2$CH$_3$)$_2$). HRMS: *m*/*z* calcd for $C_{17}H_{28}ClN_4O_9S$ [M + H]$^+$ 499.1260, found 499.1267.

Methyl (3*R*,4*R*,5*R*,6*R*)-4-Acetamido-6-acetoxy-5-azido-3-(1-ethylpropoxy)cyclohex-1-ene-1-carboxylate (10). A solution of alcohol **8** (850 mg, 2.123 mmol) and pyridine (1.71 mL, 21.23 mmol) in CH_3CN (127.0 mL) was cooled to −25 °C and added dropwise to sulfuryl chloride (0.26 mL, 3.184 mmol) over 15 min. The reaction mixture was stirred at −25 °C for 2 h, warmed to room temperature, and stirred overnight at this temperature. Excess sulfuryl chloride was decomposed by dropwise addition of EtOH (0.23 mL), and the reaction mixture was washed with 2 M sulfuric acid (200 mL). The aqueous layer was back-extracted with CH_2Cl_2 (200 mL), and the organic layers were combined and washed with water, followed by 5% aqueous $NaHCO_3$, and dried over anhydrous Na_2SO_4. Evaporation of the solvent gave the crude product, which was purified by flash column chromatography (hexanes/EtOAc 3/2) to give olefin **10** as a yellow foam (725 mg, 89% yield). $[\alpha]_D^{23}$ = −80.77° (*c* 1.3, CH_2Cl_2). ^{1}H NMR (400 MHz, $CDCl_3$): δ 6.89 (br t, $J_{2,3}$ = 1.8 Hz, 1H, H-2), 5.93 (d, $J_{4,NH}$ = 7.1 Hz, 1H, −N*H*Ac), 5.83−5.81 (m, 1H, H-6), 4.74 (dt, $J_{3,4}$ = 8.3, $J_{2,3}$ = 2.3 Hz, 1H, H-3), 4.45 (dd, $J_{4,5}$ = 11.0, $J_{5,6}$ = 7.8 Hz, 1H, H-5), 3.74 (s, 3H, −COOC*H*$_3$), 3.35 (p, *J* = 5.7 Hz, 1H, −OC*H*(CH$_2$CH$_3$)$_2$), 3.25 (dt, $J_{4,5}$ = 10.9, $J_{3,4} = J_{4,NH}$ = 7.8 Hz, 1H, H-4), 2.09 (s, 3H, −OCOC*H*$_3$), 2.03 (s, 3H, −NHCOC*H*$_3$), 1.58−1.43 (m, 4H, −OCH(C*H*$_2$CH$_3$)$_2$), 0.90 (t, *J* = 7.4 Hz, 6H, -OCH(CH$_2$C*H*$_3$)$_2$). ^{13}C NMR (100 MHz, $CDCl_3$): δ 171.1 (−NHCOCH$_3$), 169.5 (−OCOCH$_3$), 164.7 (−COOCH$_3$), 141.9 (C-2), 128.5 (C-1), 82.3 (−OCH(CH$_2$CH$_3$)$_2$), 71.8 (C-3), 69.3 (C-6), 61.5 (C-5), 56.7 (C-4), 52.2 (−COOCH$_3$), 26.1 and 25.4 (−OCH(CH$_2$CH$_3$)$_2$), 23.5 (−NHCOCH$_3$), 20.8 (−OCOCH$_3$), 9.5 and 9.3 (−OCH(CH$_2$CH$_3$)$_2$). HRMS: *m*/*z* calcd for $C_{17}H_{27}N_4O_6$ [M + H]$^+$ 383.1925, found 383.1936.

Methyl (3*R*,4*R*,5*R*,6*R*)-4-Acetamido-6-acetoxy-5-((*tert*-butoxycarbonyl)amino)-3-(1-ethylpropoxy)cyclohex-1-ene-1-carboxylate (11). The azide **10** (2.0 g, 5.233 mmol) was dissolved in THF/H_2O (5/1 v/v, 150 mL). Triphenylphosphine (2.74 g, 10.466 mmol) was added, and the mixture was heated to 50 °C for 3 h. After completion of the reaction, THF was evaporated under reduced pressure and the residue worked up with ethyl acetate and dried with Na_2SO_4. Evaporation of the solvent gave the crude product. To a stirred solution of this crude amine and Et_3N (1.45 mL, 10.46 mmol) in 50 mL of CH_2Cl_2 was added Boc_2O (3.424 g, 15.69 mmol). The reaction mixture was stirred at room temperature for overnight. The mixture was extracted with $CHCl_3$ (300 mL × 3), and the combined organic phase was washed with aqueous NH_4Cl solution, dried over Na_2SO_4, and concentrated under reduced pressure. The crude product was purified by flash chromatography (hexanes/EtOAc 2/3) to give compound **11** as a white solid (854 mg, 36% yield for two steps). $[\alpha]_D^{23}$ = −66.67° (*c* 0.3, CH_2Cl_2). ^{1}H NMR (600 MHz, $CDCl_3$): δ 6.96 (d, $J_{2,3}$ = 1.8 Hz, 1H, H-2), 6.05 (d, $J_{4,NH}$ = 9.0 Hz, 1H, −N*H*Ac), 5.86 (d, $J_{5,6}$ = 6.9 Hz, 1H, H-6), 5.24 (d, $J_{5,NH}$ = 8.9 Hz, 1H, −N*H*Boc), 4.21 (dt, $J_{4,5} = J_{4,NH}$ = 8.9, $J_{3,4}$ = 6.9 Hz, 1H, H-4), 4.03 (dt, $J_{3,4}$ = 6.5, $J_{2,3}$ = 2.3 Hz, 1H, H-3), 3.89 (dt, $J_{4,5} = J_{5,NH}$ = 9.0, $J_{5,6}$ = 7.2 Hz, 1H, H-5), 3.75 (s, 3H, −COOC*H*$_3$), 3.43 (p, *J* = 5.6 Hz, 1H, −OC*H*(CH$_2$CH$_3$)$_2$), 2.05 (s, 3H, −OCOC*H*$_3$), 1.96 (s, 3H, -NHCOC*H*$_3$), 1.55−1.48 (m, 4H, -OCH(C*H*$_2$CH$_3$)$_2$), 1.40 (s, 9H, −OC(C*H*$_3$)$_3$), 0.89 and 0.88 (t, *J* = 7.4 Hz, 3H, -OCH(CH$_2$C*H*$_3$)$_2$). ^{13}C NMR (150 MHz, $CDCl_3$): δ 170.1 (−NHCOCH$_3$), 169.4 (−OCOCH$_3$), 165.0 (−COOCH$_3$), 156.1 (−NHCOOC(CH$_3$)$_3$), 141.4 (C-2), 128.9 (C-1), 82.5 (−OCH(CH$_2$CH$_3$)$_2$), 80.0 (−OC(CH$_3$)$_3$), 74.2 (C-3), 68.3 (C-6), 53.0 (C-5), 52.5 (C-4), 52.2 (−COOCH$_3$), 28.2 (−OC(CH$_3$)$_3$), 25.8 and 25.6 (−OCH-(CH$_2$CH$_3$)$_2$), 23.3 (−NHCOCH$_3$), 20.8 (−OCOCH$_3$), 9.4 and 9.3 (−OCH(CH$_2$CH$_3$)$_2$). HRMS: *m*/*z* calcd for $C_{22}H_{36}N_2O_8Na$ [M + Na]$^+$ 479.2364, found 479.2357.

Methyl (3*R*,4*R*,5*R*,6*S*)-4-Acetamido-6-azido-5-((*tert*-butoxycarbonyl)amino)-3-(1-ethylpropoxy)cyclohex-1-ene-1-carboxylate (12). To a solution of allyl acetate **11** (700 mg, 1.533 mmol) in *t*-BuOH (20 mL) was added one portion of azidotrimethylsilane (3.024 mL, 23.0 mmol), and the reaction mixture was stirred at 80−85 °C. After 3 days, the remaining portion of azidotrimethylsilane was added to the reaction mixture and stirring was continued at the same temperature for 3 days more. The solution was poured into saturated aqueous $NaHCO_3$ and extracted with EtOAc (80 mL × 3). The combined extracts were dried over Na_2SO_4, filtered, and concentrated to afford the crude azido compound **12**. The crude product was purified by flash chromatography ($CHCl_3$/MeOH 99/1) to give the desired azido compound **12** as a white solid (310 mg, 46% yield) and 300 mg of a mixture of other products. Further purification of this mixture by flash chromatography (EtOAc/hexane 3/2) gave the azido compound **12a** (major component of the mixture) as a white solid (145 mg, 21% yield). Data for compound **12** are as follows. $[\alpha]_D^{23}$

dx.doi.org/10.1021/jo401854w | J. Org. Chem. 2013, 78, 10867−10877

= −36.67° (*c* 0.3, CH_2Cl_2). ^{1}H NMR (400 MHz, $CDCl_3$): δ 7.03 (d, $J_{2,3}$ = 4.4 Hz, 1H, H-2), 6.60 (d, $J_{4,NH}$ = 7.4 Hz, 1H, −N*H*Ac), 5.85 (d, $J_{5,NH}$ = 8.0 Hz, 1H, −N*H*Boc), 4.54 (d, $J_{5,6}$ = 2.8 Hz, 1H, H-6), 4.22 (ddd, $J_{4,NH}$ = 7.2, $J_{4,5}$ = 3.5, $J_{3,4}$ = 2.8 Hz, 1H, H-4), 4.09 (ddd, $J_{5,NH}$ = 7.9, $J_{5,6}$ = 4.0, $J_{4,5}$ = 3.7 Hz, 1H, H-5), 4.00(dd, $J_{2,3}$ = 4.1, $J_{3,4}$ = 2.7 Hz, 1H, H-3), 3.86 (s, 3H, −COOCH_3), 3.67 (p, *J* = 5.6 Hz, 1H, −OC*H*(CH_2CH_3)$_2$), 1.95 (s, 3H, −NHCOCH_3), 1.61−1.49 (m, 4H, −OCH(CH_2CH_3)$_2$), 1.41 (s, 9H, −OC(CH_3)$_3$), 0.93 and 0.89 (t, *J* = 7.4 Hz, 3H, −OCH(CH_2CH_3)$_2$). ^{13}C NMR (150 MHz, $CDCl_3$): δ 169.5 (−NHCOCH_3), 165.9 (−*C*OOCH$_3$), 154.9 (−NHCOOC(CH$_3$)$_3$), 138.1 (C-2), 128.2 (C-1), 82.4 (−O*C*H(CH_2CH_3)$_2$), 80.0 (−O*C*(CH$_3$)$_3$), 71.1 (C-3), 57.5 (C-6), 52.5 (−COO*C*H$_3$), 50.2 (C-5), 49.1 (C-4), 28.3 (−OC(*C*H$_3$)$_3$), 26.0 and 25.7 (−OCH(*C*H$_2$CH$_3$)$_2$), 23.4 (−NHCO*C*H$_3$), 9.7 and 9.0 (−OCH(*C*H$_2$CH$_3$)$_2$). HRMS: *m*/*z* calcd for $C_{20}H_{33}N_5O_6Na$ [M + Na]$^+$ 462.2323, found 462.2336. Data for methyl (3*S*,4*R*,5*S*,6*R*)-4-acetamido-6-azido-3-(*tert*-butoxycarbonylamino)-5-(1-ethylpropoxy)cyclohex-1-ene-1-carboxylate (**12a**) are as follows. ^{1}H NMR (400 MHz, $CDCl_3$): δ 7.01 (d, $J_{2,3}$ = 4.1 Hz, 1H, H-2), 5.99 (d, $J_{4,NH}$ = 8.5 Hz, 1H, −N*H*Ac), 5.22 (d, $J_{3,NH}$ = 9.6 Hz, 1H, −N*H*Boc), 4.42 (d, $J_{5,6}$ = 3.0 Hz, 1H, H-6), 4.33 (ddd, $J_{3,NH}$ = 9.6, $J_{2,3}$ = 4.8, $J_{3,4}$ = 3.4 Hz, 1H, H-3), 4.24 (ddd, $J_{4,NH}$ = 8.5, $J_{4,5}$ = 4.8, $J_{3,4}$ = 3.9 Hz, 1H, H-4), 3.84 (s, 3H, −COOCH_3), 3.77 (dd, $J_{5,6}$ = 3.6, $J_{4,5}$ = 4.8 Hz, 1H, H-5), 3.41 (p, *J* = 5.5 Hz, 1H, −OC*H*(CH_2CH_3)$_2$), 1.95 (s, 3H, −NHCOCH_3), 1.60−1.45 (m, 4H, −OCH(CH_2CH_3)$_2$), 1.42 (s, 9H, −OC(CH_3)$_3$), 0.89 and 0.85 (t, *J* = 7.4 Hz, 3H, −OCH(CH_2CH_3)$_2$). ^{13}C NMR (150 MHz, $CDCl_3$): δ 169.7 (−NHCOCH_3), 166.1 (−*C*OOCH$_3$), 155.0 (−NHCOOC(CH$_3$)$_3$), 139.8 (C-2), 127.7 (C-1), 83.1 (−O*C*H(CH_2CH_3)$_2$), 80.1 (−O*C*(CH$_3$)$_3$), 75.0 (C-5), 58.2 (C-6), 52.5 (−COO*C*H$_3$), 50.6 (C-4), 48.7 (C-3), 28.4 (−OC(*C*H$_3$)$_3$), 25.8 and 25.7 (−OCH(*C*H$_2$CH$_3$)$_2$), 23.4 (−NHCO*C*H$_3$), 9.5 and 9.2 (−OCH(*C*H$_2$CH$_3$)$_2$). HRMS: *m*/*z* calcd for $C_{20}H_{33}N_5O_6Na$ [M + Na]$^+$ 462.2323, found 462.2309.

Methyl (3*R*,4*R*,5*R*,6*S*)-4-Acetamido-5-((*tert*-butoxycarbonyl)amino)-3-(1-ethylpropoxy)-6-[4-(1-hydroxypropyl)[1,2,3]-triazol-1-yl]-cyclohex-1-ene-1-carboxylate (13). To a stirred solution of azide **12** (200 mg, 0.455 mmol) and pent-1-yn-3-ol (51.0 μL, 0.6 mmol) in a 1/1 mixture (4 mL) of water and *tert*-butyl alcohol was added copper(II) sulfate pentahydrate (8.0 mg) followed by the addition of a freshly prepared 1 M solution (0.16 mL) of sodium ascorbate in water. The reaction went to completion after vigorous stirring at room temperature for 4 h. The reaction mixture was diluted with CH_2Cl_2 (150 mL) and washed with 10% NH_4OH (70 mL × 2) and water (70 mL × 2). The organic layer was dried over anhydrous Na_2SO_4, concentrated to dryness, and purified by flash chromatography ($CHCl_3$/MeOH 19/1) to give triazole **13** (170 mg, 71% yield) as a white solid. Data for the mixture of diastereomers are as follows. ^{1}H NMR (600 MHz, $CDCl_3$): δ 7.82 (s, 2H, H-5′), 7.45−7.40 (br m, 2H, −N*H*Ac), 7.24 (d, $J_{2,3}$ = 3.8 Hz, 2H, H-2), 6.10 (d, *J* = 6.8 Hz, 2H, −N*H*Boc), 5.40 (s, 2H, H-6), 4.82−4.78 (m, 2H, −C*H*(OH)CH$_2$CH$_3$), 4.45−4.42 (m, 2H, H-4), 4.22−4.20 (m, 2H, H-3), 4.10−4.07 (m, 2H, H-5), 3.65 (s, 6H, −COOCH_3), 3.62−3.59 (m, 2H, −OC*H*(CH$_2$CH$_3$)$_2$), 1.94−1.84 (m, 4H, −CH(OH)CH_2CH$_3$), 1.87 (s, 6H, -NHCOCH_3), 1.63−1.55 (m, 8H, -OCH(CH_2CH$_3$)$_2$), 1.39 (s, 18H, −OC(CH_3)$_3$), 0.97−0.93 (m, 12H, −CH(OH)CH$_2$CH_3, −OCHCH$_2$CH_3), 0.91 (t, *J* = 7.5 Hz, 6H, −OCHCH$_2$CH_3). ^{13}C NMR (150 MHz, $CDCl_3$): δ 170.0 (−NHCOCH$_3$), 165.0 and 164.9 (−*C*OOCH$_3$), 155.2 (−NHCOOC(CH$_3$)$_3$), 151.3 (C-4′), 140.0 (C-2), 127.2 (C-1), 123.0 (C-5′), 82.7 (−OCH(CH$_2$CH$_3$)$_2$), 80.1 (−O*C*(CH$_3$)$_3$), 72.1 (2C, C-3), 68.2 (−*C*H(OH)CH$_2$CH$_3$), 58.2 (C-6), 53.4 (C-5), 52.4 (−COO*C*H$_3$), 48.4 (C-4), 30.3 and 30.2 (−CH(OH)*C*H$_2$CH$_3$)$_2$), 28.3 (−OC(*C*H$_3$)$_3$), 25.8 and 25.7 (−OCH(*C*H$_2$CH$_3$)$_2$), 23.1 (−NHCO*C*H$_3$), 9.7 and 9.6 (−CH(OH)CH$_2$*C*H$_3$), 9.5 and 9.1 (−OCH(*C*H$_2$CH$_3$)$_2$). HRMS: *m*/*z* calcd for $C_{25}H_{41}N_5O_7Na$ [M + Na]$^+$ 546.2898, found 546.2906.

(3*R*,4*R*,5*R*,6*S*)-4-Acetamido-5-((*tert*-butoxycarbonyl)amino)-3-(1-ethylpropoxy)-6-[4-(1-hydroxypropyl)[1,2,3]-triazol-1-yl]-cyclohex-1-ene-1-carboxylic Acid (14). KOH (1 N, 3.0 mL) was added to a solution of compound **13** (100 mg, 0.191 mmol) in 10 mL of THF, and the reaction mixture was stirred at room temperature overnight. The pH of the reaction mixture was adjusted to 7 by bubbling CO_2, and the solvents were evaporated. The crude mass was purified by flash column chromatography ($CHCl_3$/MeOH, 3/1 (v/v)), and the resulting carboxylic acid (oil-like compound) was dissolved in a minimum amount of MeOH and EtOAc (1−2 mL). The desired acid was precipitated out in this solution, and the precipitate was filtered and dried to give the pure carboxylic acid **14** (46 mg, 47% yield) as a white solid. Data for the mixture of diastereomers: ^{1}H NMR (600 MHz, CD_3OD): δ 7.80 (d like, 2H, H-5′), 7.01 (d, $J_{2,3}$ = 1.7 Hz, 2H, H-2), 5.51−5.46 (m, 2H, H-6), 4.70 (dt, *J* = 13.1, 6.5 Hz, 2H, −C*H*(OH)CH$_2$CH$_3$), 4.38 (d, $J_{3,4}$ = 7.9 Hz, 2H, H-4), 4.15−4.02 (m, 4H, H-4, H-5), 3.48 (p, *J* = 5.6 Hz, 2H, −OC*H*(CH$_2$CH$_3$)$_2$), 1.95 (d like, 6H, −NHCOCH_3), 1.90−1.77 (m, 4H, −CH(OH)CH_2CH$_3$), 1.60−1.49 (m, 8H, −OCH(CH_2CH$_3$)$_2$), 1.32 (d like, 18H, −OC(CH_3)$_3$), 0.96 (t, *J* = 7.4 Hz, 6H, −OCHCH$_2$CH_3), 0.91−0.88 (m, 12H, −CH(OH)CH$_2$CH_3, −OCHCH$_2$CH_3). ^{13}C NMR (150 MHz, MeOD): δ 173.6 (−NHCOCH$_3$), 167.5 (2C, −*C*OOH), 157.6 (2C, −NHCOOC(CH$_3$)$_3$), 152.1 and 151.9 (C-4′), 143.6 (2C, C-2), 130.0 (C-1), 124.1 (2C, C-5′), 84.1 (2C, −OCH(CH$_2$CH$_3$)$_2$), 80.4 (2C, −O*C*(CH$_3$)$_3$), 76.1 (C-3), 69.1 and 69.0 (−*C*H(OH)CH$_2$CH$_3$), 62.8 (2C, C-6), 57.1 and 57.0 (C-5), 55.6 and 55.5 (C-4), 31.5 and 31.32 (−CH(OH)*C*H$_2$CH$_3$), 28.6 (−OC(*C*H$_3$)$_3$), 27.2 and 26.6 (−OCH(*C*H$_2$CH$_3$)$_2$), 22.9 (2C, −NHCO*C*H$_3$), 10.0, 9.9, and 9.6 (−OCH(*C*H$_2$CH$_3$)$_2$, −CH(OH)CH$_2$*C*H$_3$). HRMS: *m*/*z* calcd for $C_{24}H_{40}N_5O_7$ [M + H]$^+$ 510.2922, found 510.2924.

(3*R*,4*R*,5*R*,6*S*)-4-Acetamido-5-amino-3-(1-ethylpropoxy)-6-[4-(1-hydroxypropyl)[1,2,3]-triazol-1-yl]cyclohex-1-ene-1-carboxylic Acid Trifluoroacetate Salt (5). The carboxylic acid **14** (20 mg) was dissolved in a 1/3 mixture of TFA and dichloromethane (1 mL), and this mixture was stirred at room temperature for 3 h. Solvents were evaporated, and the crude mass was then triturated with dichloromethane (2 × 2 mL) to yield compound **5** as a colorless foam (18 mg, 88% yield). Data for the mixture of diastereomers are as follows. ^{1}H NMR (600 MHz, D_2O): δ 8.11 (d like, 2H, H-5′), 7.16 (d, $J_{2,3}$ = 2.3 Hz, 2H, H-2), 6.01−5.98 (m, 2H, H-6), 4.83 (t, *J* = 6.8 Hz, 2H, −C*H*(OH)CH$_2$CH$_3$), 4.61 (d, $J_{3,4}$ = 9.1 Hz, 2H, H-3), 4.37 (dd, $J_{3,4}$ = 9.2, $J_{4,5}$ = 11.9 Hz, 2H, H-4), 4.17−4.12 (m, 2H, H-5), 3.62 (p, *J* = 5.6 Hz, 2H, −OC*H*(CH$_2$CH$_3$)$_2$), 2.10 (s, 6H, −NHCOCH_3), 1.90−1.84 (m, 4H, −CH(OH)CH_2CH$_3$), 1.64−1.47 (m, 8H, −OCH(CH_2CH$_3$)$_2$), 0.91 (t, *J* = 7.4 Hz, 6H, −OCHCH$_2$CH_3), 0.88−0.85 (m, 12H, −CH(OH)CH$_2$CH_3, -OCHCH$_2$CH_3). ^{13}C NMR (150 MHz, D_2O): δ 175.5 (−NHCOCH$_3$), 166.5 (−COOH), 163.0 (q, $J_{C,F}$ = 35.3 Hz, CF_3COO^-), 151.1 (2C, C-4′), 143.2 (2C, C-2), 126.9 and 126.8 (C-1), 123.8 and 123.5 (C-5′), 116.4 (q, $J_{C,F}$ = 289.4 Hz, CF_3COO^-), 84.7 (−OCH(CH$_2$CH$_3$)$_2$), 73.7 (C-3), 67.4 (2C, −CH(OH)CH$_2$CH$_3$), 59.4 (C-6), 54.4 (2C, C-5), 51.8 (2C, C-4), 29.2 (−CH(OH)*C*H$_2$CH$_3$), 25.3 and 24.9 (−OCH(*C*H$_2$CH$_3$)$_2$), 22.5 (−NHCO*C*H$_3$), 8.9, 8.5, and 8.4 (−OCH(CH$_2$*C*H$_3$)$_2$, −CH(OH)CH$_2$*C*H$_3$). HRMS: *m*/*z* calcd for $C_{19}H_{32}N_5O_5$ [M + H]$^+$ 410.2398, found 410.2404.

Methyl (3*R*,4*R*,5*R*,6*S*)-4-Acetamido-5-amino-3-(1-ethylpropoxy)-6-[4-(1-hydroxypropyl)[1,2,3]-triazol-1-yl]cyclohex-1-ene-1-carboxylate Trifluoroacetate Salt (15). The methyl ester **13** (30 mg) was dissolved in a 1/2 mixture of TFA and dichloromethane (2 mL) and stirred at room temperature for 3 h. Solvents were evaporated, and the crude mass was then dissolved in EtOAc and allowed to precipitate. The precipitate was filtered and dried to give compound **15** as a white solid (19 mg, 62% yield). Data for the mixture of diastereomers are as follows. ^{1}H NMR (600 MHz, D_2O): δ 8.17 (d like, *J* = 8.8 Hz, 2H, H-5′), 7.22−7.20 (m, 2H, H-2), 6.06−6.04 (m, 2H, H-6), 4.87 (td, *J* = 6.7, 2.8 Hz, 2H, −C*H*(OH)CH$_2$CH$_3$), 4.65 (d, $J_{3,4}$ = 9.2 Hz, 2H, H-3), 4.40 (dd, $J_{3,4}$ = 9.3, $J_{4,5}$ = 11.9 Hz, 2H, H-4), 4.19 (ddd, $J_{4,5}$ = 12.0, $J_{5,NH}$ = 9.2, $J_{5,6}$ = 4.4 Hz, 2H, H-5), 3.66 (p, *J* = 5.6 Hz, 2H, −OC*H*(CH$_2$CH$_3$)$_2$), 3.62 (s, 6H, −COOCH_3), 2.13 (s, 6H, −NHCOCH_3), 1.94−1.88 (m, 4H, −CH(OH)CH_2CH$_3$), 1.68−1.51 (m, 8H, −OCH(CH_2CH$_3$)$_2$), 0.94 (t, *J* = 7.4 Hz, 6H, −OCHCH$_2$CH_3), 0.92−0.89 (m, 12H, −CH(OH)CH$_2$CH_3, −OCHCH$_2$CH_3). ^{13}C NMR (150 MHz, D_2O): δ 175.4 (−NHCOCH$_3$), 165.2 (−COOH), 162.9 (q, $J_{C,F}$ = 35.3 Hz, CF_3COO^-), 151.2 (2C, C-4′), 143.6 and 143.5 (C-2), 126.2

dx.doi.org/10.1021/jo401854w | *J. Org. Chem.* 2013, 78, 10867−10877

and 126.1 (C-1), 123.8 and 123.5 (C-5′), 116.4 (q, $J_{C,F}$ = 290.0 Hz, CF_3COO^-), 84.6 ($-OCH(CH_2CH_3)_2$), 73.7 (2C, C-3), 67.4 and 67.3 ($-CH(OH)CH_2CH_3$), 59.3 (C-6), 54.3 (2C, C-5), 52.9 ($-COOCH_3$), 51.8 and 51.7 (C-4), 29.2 and 29.1 ($-CH(OH)CH_2CH_3$), 25.3 and 24.9 ($-OCH(CH_2CH_3)_2$), 22.4 ($-NHCOCH_3$), 8.9 ($-CH(OH)CH_2CH_3$), 8.5 and 8.4 ($-OCH(CH_2CH_3)_2$). HRMS: *m*/*z* calcd for $C_{20}H_{34}N_5O_5$ $[M + H]^+$ 424.2554, found 424.2561.

Methyl (3*R*,4*R*,5*R*,6*S*)-4-Acetamido-5-(2,3-bis(*tert*-butoxycarbonyl)guanidino)-3-(1-ethylpropoxy)-6-(4-(1-hydroxypropyl)[1,2,3]-triazol-1-yl]cyclohex-1-ene-1-carboxylate (16). The methyl ester **13** (90 mg) was dissolved in a 1/2 mixture of TFA and dichloromethane (4 mL) and stirred at room temperature for 3 h. Solvents were evaporated, the crude mass was then dissolved in MeOH (4 mL), and the pH of this solution was adjusted to 7 by adding Amberlyst A26 (nearly 200 mg). The resin was removed by filtration, and the filtrate was concentrated to obtain the free amine (62 mg, 87% yield) as a light yellow liquid. To a stirred solution of this free amine (62 mg, 0.146 mmol), *N*,*N*′-bis(*tert*-butoxycarbonyl)-thiourea (60.7 mg, 0.219 mmol), and Et_3N (0.04 mL, 0.292 mmol) in dry DMF (9 mL) at 0 °C was added $HgCl_2$ (60 mg, 0.219 mmol). After the addition, the reaction temperature was maintained at 0 °C for 1 h and then warmed to room temperature overnight. The reaction mixture was then diluted with ethyl acetate and filtered. The filtrate was concentrated to dryness and purified by flash column chromatography (MeOH/$CHCl_3$ 1/9) to give compound **16** (84 mg, 86% yield) as a colorless liquid. Data for the mixture of diastereomers are as follows. ^{1}H NMR (600 MHz, MeOD): δ 8.03 (d like, J = 9.7 Hz, 2H, H-5′), 7.18−7.17 (m, 2H, H-2), 5.77−5.72 (m, 2H, H-6), 4.74−4.61 (m, 4H, H-5, $-CH(OH)CH_2CH_3$), 4.37−4.34 (m, 2H, H-3), 4.31−4.28 (m, 2H, H-4), 3.60 (d like, 6H, $-COOCH_3$), 3.51 (p, J = 5.5 Hz, 2H, $-OCH(CH_2CH_3)_2$), 1.86−1.76 (m, 4H, $-CH(OH)CH_2CH_3$), 1.81 (s, 6H, $-NHCOCH_3$), 1.65−1.56 (m, 8H, $-OCH(CH_2CH_3)_2$), 1.53 (d like, 18H, $-OC(CH_3)_3$), 1.44 (d like, 18H, $-OC(CH_3)_3$), 0.95 (t, J = 7.6 Hz, 6H, $-OCHCH_2CH_3$), 0.94−0.84 (m, 12H, $-OCHCH_2CH_3$, $-CH(OH)CH_2CH_3$). ^{13}C NMR (150 MHz, MeOD): δ 173.2 ($-NHCOCH_3$), 166.3 and 166.2 ($-COOCH_3$), 164.1 (2C, $-NCOOC(CH_3)_3$), 157.7 (2C, $-C{=}N$), 153.5 (2C, $-NHCOOC(CH_3)_3$), 152.6 and 152.5 (C-4′), 143.2 and 143.1 (C-2), 128.5 (2C, C-1), 124.0 and 123.9 (C-5′), 84.8 and 84.7 ($-OCH(CH_2CH_3)_2$), 84.7 ($-OC(CH_3)_3$), 80.6 and 80.5 ($-OC(CH_3)_3$), 75.0 and 74.9 (C-3), 68.9 (2C, $-CH(OH)CH_2CH_3$), 61.0 and 60.8 (C-6), 55.7 and 55.6 (C-5), 53.3 (C-4), 52.7 ($-COOCH_3$), 31.5 and 31.4 ($-CH(OH)CH_2CH_3$), 28.5 (2C, $-OC(CH_3)_3$), 28.2 (2C, $-OC(CH_3)_3$), 27.2 and 26.8 ($-OCH(CH_2CH_3)_2$), 22.7 ($-NHCOCH_3$), 10.1, 10.0, 9.9, 9.7, and 9.6 ($-OCH(CH_2CH_3)_2$, $-CH(OH)CH_2CH_3$). HRMS: *m*/*z* calcd for $C_{31}H_{52}N_7O_9$ $[M + H]^+$ 666.3821, found 666.3825.

Methyl (3*R*,4*R*,5*R*,6*S*)-4-Acetamido-3-(1-ethylpropoxy)-5-guanidino-6-[4-(1-hydroxypropyl)[1,2,3]-triazol-1-yl]cyclohex-1-ene-1-carboxylate Trifluoroacetate Salt (17). The guanidinium compound **16** (12 mg) was dissolved in a 1/1 mixture of TFA and dichloromethane (1 mL) and stirred at room temperature for 3 h. Solvents were evaporated, and the crude mass was then triturated with dichloromethane (2 × 2 mL) to give compound **17** as a colorless liquid (10 mg, 96% yield). Data for the mixture of diastereomers are as follows. ^{1}H NMR (600 MHz, D_2O): δ 8.09 (d like, 2H, H-5′), 7.19 (d, $J_{4,5}$ = 1.3 Hz, 2H, H-2), 5.79−5.74 (m, 2H, H-6), 4.89−4.82 (m, 2H, $-CH(OH)CH_2CH_3$), 4.66 (br s, 2H, H-3), 4.23 (br s, 4H, H-4, H-5), 3.66−3.63 (m, 2H, $-OCH(CH_2CH_3)_2$), 3.62 (d like, 6H, $-COOCH_3$), 2.05 (s, 6H, $-NHCOCH_3$), 1.92−1.85 (m, 4H, $-CH(OH)CH_2CH_3$), 1.67−1.48 (m, 8H, $-OCH(CH_2CH_3)_2$), 0.94 and 0.88 (t, J = 7.4 Hz, 6H, $-OCH(CH_2CH_3)_2$), 0.84 and 0.83 (t, J = 7.4, 3H, $-CH(OH)CH_2CH_3$). ^{13}C NMR (150 MHz, D_2O): δ 174.4 ($-NHCOCH_3$), 165.2 (2C, $-COOCH_3$), 162.4 (q, J = 35.6 Hz, CF_3COO^-), 156.4 and 156.3 ($-C{=}N$), 150.5 and 150.3 (C-4′), 143.1 (C-2), 126.2 (2C, C-1), 123.2 (2C, C-5′), 115.9 (q, J = 291.7 Hz, CF_3COO^-), 84.2 ($-OCH(CH_2CH_3)_2$), 73.9 (C-3), 66.9 and 66.7 ($-CH(OH)CH_2CH_3$), 61.0 (2C, C-6), 56.5 (C-5), 53.0 (C-4), 52.3 ($-COOCH_3$), 28.8 and 28.7 ($-CH(OH)CH_2CH_3$), 25.0 and, 24.5 ($-OCH(CH_2CH_3)_2$), 21.4 ($-NHCOCH_3$), 8.2, 8.1, and 7.9 ($-OCH(CH_2CH_3)_2$, $-CH(OH)CH_2CH_3$). HRMS: *m*/*z* calcd for $C_{21}H_{36}N_7O_5$ $[M + H]^+$ 466.2772, found 466.2783.

(3*R*,4*R*,5*R*,6*S*)-4-Acetamido-3-(1-ethylpropoxy)-5-guanidino-6-(4-(1-hydroxypropyl)[1,2,3]-triazol-1-yl]cyclohex-1-ene-1-carboxylic Acid Trifluoroacetate Salt (6). To a stirred solution of ammonium salt **5** (17 mg, 0.0325 mmol) and Et_3N (0.045 mL, 0.325 mmol) in dry MeOH (1 mL) was added *N*,*N*′-Di-Boc-1*H*-pyrazole-1-carboxamidine (31.0 mg, 0.1 mmol). After the addition, the reaction mixture was stirred at room temperature for 3−4 days. MeOH was evaporated, and the crude product was purified by flash chromatography (EtOAc/MeOH/H_2O (3/1) 9:1) to give the desired guanidinium compound as a liquid (7 mg, 33% yield). Then the guanidinium compound (5.0 mg) was dissolved in a 1/2 mixture of TFA and dichloromethane (1.2 mL) and stirred at room temperature for 3 h. Solvents were evaporated, and the crude mass was then triturated with dichloromethane (2 × 1 mL) to give compound **6** as a colorless liquid. Data for the mixture of diastereomers are as follows. ^{1}H NMR (600 MHz, D_2O): δ 8.05 (d like, 2H, H-5′), 7.09 (s, 2H, H-2), 5.73 (s, 2H, H-6), 4.88−4.83 (m, 2H, $-CH(OH)CH_2CH_3$), 4.64 (br s, 2H, H-3), 4.21 (br s, 4H, H-4, H-5), 3.67−3.63 (m, 2H, $-OCH(CH_2CH_3)_2$), 2.06 (d like, 6H, $-NHCOCH_3$), 1.92−1.86 (m, 4H, $-CH(OH)CH_2CH_3$), 1.68−1.49 (m, 8H, $-OCH(CH_2CH_3)_2$), 0.95 and 0.89 (t, J = 7.3 Hz, 6H, $-OCH(CH_2CH_3)_2$), 0.84 (t, J = 7.4 Hz, 6H, $-CH(OH)CH_2CH_3$). ^{13}C NMR (150 MHz, D_2O): δ 174.4 ($-NHCOCH_3$), 167.3 ($-COOH$), 162.5 (q, J = 34.8 Hz), 156.4 and 156.3 ($-C{=}N$), 150.4 and 150.2 (C-4′), 141.3 (C-1), 128.1 (C-2), 123.0 and 122.9 (C-5′), 115.9 (q, J = 291.0 Hz, CF_3COO^-), 84.2 ($-OCH(CH_2CH_3)_2$), 74.1 (C-3), 66.9 and 66.8 ($-CH(OH)CH_2CH_3$), 61.4 and 61.3 (C-6), 56.5 (C-5), 53.1 (C-4), 28.8 and 28.7 ($-CH(OH)CH_2CH_3$), 25.0 and 24.6 ($-OCH(CH_2CH_3)_2$), 21.4 ($-NHCOCH_3$), 8.2, 8.1, 8.1, and 8.0 ($-OCH(CH_2CH_3)_2$, $-CH(OH)CH_2CH_3$). In addition to the resonances of the desired compound, a triplet and quartet were also observed at 1.30 and 3.22 ppm, respectively, resulting from CF_3COOEt_3NH salt contamination (4.0 mg, containing 12.5 wt % of triethylammonium trifluoroacetate by ^{1}H NMR, 80% yield after correcting for salt content). HRMS: *m*/*z* calcd for $C_{20}H_{34}N_7O_5$ $[M + H]^+$ 452.2616, found 452.2617.

■ ASSOCIATED CONTENT

Ⓢ Supporting Information

Figures and tables giving ^{1}H and ^{13}C NMR spectra, NOE spectra, and further details from MD simulations. This material is available free of charge via the Internet at http://pubs.acs.org.

■ AUTHOR INFORMATION

Corresponding Author

*B.M.P.: tel, +1 778 782 4152; fax, +1 778 782 4860; e-mail, bpinto@sfu.ca.

Notes

The authors declare no competing financial interest.

■ ACKNOWLEDGMENTS

We are grateful to the Natural Sciences and Engineering Research Council of Canada for financial support. We thank one of the reviewers for insightful suggestions. MD computations were performed on the Western Canada Research Grid.

■ REFERENCES

(1) (a) Glezen, W. P. *Epidemiol. Rev.* **1982**, *4*, 25−44. (b) Monto, A. S.; Iacuzio, I. A.; LaMontague, J. R. *J. Infect. Dis.* **1997**, *176*, S1−S3. (c) Service, R. F. *Science* **1997**, *275*, 756−757. (d) Thompson, W. W.; Comanor, L.; Shay, D. K. *J. Infect. Dis.* **2006**, *194*, S82−S91.

(2) (a) Schmidt, A. C. *Drugs* **2004**, *64*, 2031−2046. (b) De Clercq, E. *Nat. Rev. Drug Discovery* **2006**, *5*, 1015−1025.

(3) (a) Kim, C. U.; Lew, W.; Williams, M. A.; Liu, H.; Zhang, L.; Swaminathan, S.; Bischofberger, N.; Chen, M. S.; Mendel, D. B.; Tai,

C. Y.; Laver, W. G.; Stevens, R. C. *J. Am. Chem. Soc.* **1997**, *119*, 681−690. (b) McClellan, K.; Perry, C. M. *Drugs* **2001**, *61*, 263−283.
(4) (a) von Itzstein, M.; Wu, W.-Y.; Kok, G. B.; Pegg, M. S.; Dyason, J. C.; Jin, B.; Phan, T. V.; Smythe, M. L.; White, H. F.; Oliver, S. W.; Colman, P. M.; Varghese, J. N.; Ryan, D. M.; Woods, J. M.; Bethell, R. C.; Hotham, V. J.; Cameron, J. M.; Penn, C. R. *Nature* **1993**, *363*, 418−423. (b) Dunn, C. J.; Goa, K. L. *Drugs* **1999**, *58*, 761−784.
(5) (a) Jain, S.; Fry, A. M. *Clin. Infect. Dis.* **2011**, *52*, 707−709. (b) Kubo, S.; Tomozawa, T.; Kakuta, M.; Tokumitsu, A.; Yamashita, M. *Antimicrob. Agents Chemother.* **2010**, *54*, 1256−1264.
(6) (a) Le, Q. M.; Kiso, M.; Someya, K.; Sakai, Y. T.; Nguyen, T. H.; Nguyen, K. H. L.; Pham, N. D.; Ngyen, H. H.; Yamada, S.; Muramoto, Y.; Horimoto, T.; Takada, A.; Goto, H.; Suzuki, T.; Suzuki, Y.; Kawaoka, Y. *Nature* **2005**, *437*, 1108−1108. (b) Chen, H.; Cheung, C. L.; Tai, H.; Zhao, P.; Chan, J. F.W.; Cheng, V. C.C.; Chan, K.-H.; Yuen, K.-Y. *Emerg. Infect. Dis.* **2009**, *15*, 1970−1972. (c) Seibert, C. W.; Rahmat, S.; Krammer, F.; Palese, P.; Bouvier, N. M. *J. Virol.* **2012**, *86*, 5386−5389.
(7) Thompson, J. D.; Higgins, D. G.; Gibson, T. J. *Comput. Appl. Biosci.* **1994**, *10*, 19−29.
(8) (a) Russell, R. J.; Haire1, L. F.; Stevens, D. J.; Collins, P. J.; Lin, Y. P.; Blackburn, G. M.; Hay, A. J.; Gamblin, S. J.; Skehel, J. J. *Nature* **2006**, *443*, 45−49. (b) Li, Q.; Qi, J.; Zhang, W.; Vavricka, C. J.; Shi, Y.; Wei, J.; Feng, E.; Shen, J.; Chen, J.; Liu, D.; He, J.; Yan, J.; Liu, H.; Jiang, H.; Teng, M.; Li, X.; Gao, G. F. *Nat. Struct. Mol. Biol.* **2010**, *17*, 1266−1268.
(9) (a) Rudrawar, S.; Dyason, J. C.; Rameix-Welti, M.-A.; Rose, F. J.; Kerry, P. S.; Russell, R. J. M.; van der Werf, S.; Thomson, R. J.; Naffakh, N.; von Itzstein, M. *Nat. Commun.* **2010**, *1*, 113. (b) Wen, W.-H.; Wang, S.-Y.; Tsai, K.-C.; Cheng, Y.-S. E.; Yang, A.-S.; Fanga, J.-M.; Wong, C.-H. *Bioorg. Med. Chem.* **2010**, *18*, 4074−4084. (c) Ye, D.; Shin, W.-J.; Li, N.; Tang, W.; Feng, E.; Li, J.; He, P.-L.; Zuo, J.-P.; Kim, H.; Nam, K.-Y.; Zhu, W.; Seong, B.-L.; No, K. T.; Jiang, H.; Liu, H. *Eur. J. Med. Chem.* **2012**, *54*, 764−770. (d) Du, J.; Cross, T. A.; Zhou, H.-X. *Drug Discovery Today* **2012**, *17*, 19−20.
(10) Wu, Y.; Qin, G.; Gao, F.; Liu, Y.; Vavricka, C. J.; Qi, J.; Jiang, H.; Yu, K.; Gao, G. F. *Sci. Rep.* **2013**, *3*, 1551.
(11) (a) Amaro, R. E.; Minh, D. D. L.; Cheng, L. S.; Lindstrom, W. M., Jr.; Olson, A. J.; Lin, J.-H.; Li, W. W.; McCammon, J. A. *J. Am. Chem. Soc.* **2007**, *129*, 7764−7765. (b) Cheng, X.; Ivanov, I.; Xu, D.; McCammon, J. *J. Am. Chem. Soc.* **2009**, *131*, 4702−4709. (c) Amaro, R. E.; Swift, R. V.; Votapka, L.; Li, W. W.; Walker, R. C.; Bush, R. M. *Nat. Commun.* **2011**, *2*, 388.
(12) (a) Mohan, S.; McAtamney, S.; Haselhorst, T.; von Itzstein, M.; Pinto, B. M. *J. Med. Chem.* **2010**, *53*, 7377−7391. (b) Niikura, M.; Bance, N.; Mohan, S.; Pinto, B. M. *Antiviral Res.* **2011**, *90*, 160−163. (c) Albohy, A.; Mohan, S.; Zheng, R. B.; Pinto, B. M.; Cairo, C. W. *Bioorg. Med. Chem.* **2011**, *19*, 2817−2822. (d) Greenway, K. T.; LeGresley, E. B.; Pinto, B. M. *PloS ONE* **2013**, *8*, e59873. (e) Kerry, P. S.; Mohan, S.; Russell, R. J. M.; Bance, N.; Niikura, M.; Pinto, B. M. *Sci. Rep.* **2013**, DOI: 10.1038/srep02871.
(13) Hata, K.; Koseki, K.; Yamaguchi, K.; Moriya, S.; Suzuki, Y.; Yingsakmongkon, S.; Hirai, G.; Sodeoka, M.; von Itzstein, M.; Miyagi, T. *Antimicrob. Agents Chemother.* **2008**, *52*, 3484−3491.
(14) (a) Pal, A. P. J.; Gupta, P.; Reddy, Y. S.; Vankar, Y. D. *Eur. J. Org. Chem.* **2010**, 6957−6966. (b) Plietker, B.; Niggemann, M. *J. Org. Chem.* **2005**, *70*, 2402−2405. (c) Tiwari, P.; Misra, A. K. *J. Org. Chem.* **2006**, *71*, 2911−2913.
(15) Martin, J. C.; Arhar, R. J. *J. Am. Chem. Soc.* **1971**, *93*, 4327−4329.
(16) Burgess, E. M.; Penton, H. A.; Taylor, E. A., Jr. *J. Org. Chem.* **1973**, *38*, 26−31.
(17) Barrett, A. G. M.; Braddock, D. C.; James, R. A.; Koike, N.; Procopiou, P. A. *J. Org. Chem.* **1998**, *63*, 6273−6280.
(18) (a) Begum, L.; Box, J. M.; Drew, M. G. B.; Harwood, L. M.; Humphreys, J. L.; Lowes, D. J.; Morris, G. A.; Redon, P. M.; Walkerb, F. M.; Whitehea, R. C. *Tetrahedron* **2003**, *59*, 4827−4841. (b) Prazeres, V. F. V.; Castedo, L.; González-Bello, C. *Eur. J. Org. Chem.* **2008**, 3991−4003.
(19) (a) Boyd, D. R.; Sharma, N. D.; Belhocine, T.; Malone, J. F.; McGregor, S. T.; Atchison, J.; Mclntyre, P. A. B.; Stevenson, P. J. *J. Phys. Org. Chem.* **2013**, and references therein DOI: 10.1002/poc.3183. (b) Ferrier, R. J.; Vethaviyaser, N. *J. Chem. Soc. C* **1971**, 1907−1913.
(20) Thirumurugan, P.; Matosiuk, D.; Jozwiak, K. *Chem. Rev.* **2013**, *113*, 4905−4979.
(21) Trott, O.; Olson, A. J. *J. Comput. Chem.* **2010**, *31*, 455−461.
(22) Venkatramani, L.; Bochkareva, E.; Lee, J. T.; Gulati, U.; Laver, G.; Bochkarev, W. A.; Air, G. M. *J. Mol. Biol.* **2006**, *356*, 651−663.
(23) Chen, V. B.; Arendall, W. B.; Headd, J. J.; Keedy, D. A.; Immormino, R. M.; Kapral, G. J.; Murray, M. W.; Richardson, J. S.; Richardson, D. C. *Acta Crystallogr., Sect. D: Biol. Crystallogr.* **2010**, *66*, 12−21.
(24) Dolinsky, T. J.; Czodrowski, P.; Li, H.; Nielsen, J. E; Jensen, J. H.; Klebe, G.; Baker, N. A. *Nucleic Acids Res.* **2007**, *35*, W522−W525.
(25) Lawrenz, M.; Wereszczynski, J.; Amaro, R.; Walker, R.; Roitberg, A.; McCammon, J. A. *Bioinformatics* **2010**, *78*, 2523−2532.
(26) Case, D. A.; Cheatham, T. E.; Darden, T.; Gohlke, H.; Luo, R.; Merz, K. M., Jr.; Onufriev, A.; Simmerling, C.; Wang, B.; Woods, R. J. *J. Comput. Chem.* **2005**, *26*, 1668−1688.
(27) Cornell, W. D.; Cieplak, P.; Bayly, C. I.; Gould, I. R.; Merz, K. M.; Ferguson, D. M.; Spellmeyer, D. C.; Fox, T.; Caldwell, J. W.; Kollman, P. A. *J. Am. Chem. Soc.* **1995**, *117*, 5179−5197.
(28) Frisch, M. J.; Trucks, G. W.; Schlegel, H. B.; Scuseria, G. E.; Robb, M. A.; Cheeseman, J. R.; Scalmani, G.; Barone, V.; Mennucci, B.; Petersson, G. A.; Nakatsuji, H.; Caricato, M.; Li, X.; Hratchian, H. P.; Izmaylov, A. F.; Bloino, J.; Zheng, G.; Sonnenberg, J. L.; Hada, M.; Ehara, M.; Toyota, K.; Fukuda, R.; Hasegawa, J.; Ishida, M.; Nakajima, T.; Honda, Y.; Kitao, O.; Nakai, H.; Vreven, T.; Montgomery, J. A., Jr.; Peralta, J. E.; Ogliaro, F.; Bearpark, M.; Heyd, J. J.; Brothers, E.; Kudin, K. N.; Staroverov, V. N.; Kobayashi, R.; Normand, J.; Raghavachari, K.; Rendell, A.; Burant, J. C.; Iyengar, S. S.; Tomasi, J.; Cossi, M.; Rega, N.; Millam, J. M.; Klene, M.; Knox, J. E.; Cross, J. B.; Bakken, V.; Adamo, C.; Jaramillo, J.; Gomperts, R.; Stratmann, R. E.; Yazyev, O.; Austin, A. J.; Cammi, R.; Pomelli, C.; Ochterski, J. W.; Martin, R. L.; Morokuma, K.; Zakrzewski, V. G.; Voth, G. A.; Salvador, P.; Dannenberg, J. J.; Dapprich, S.; Daniels, A. D.; Farkas, Ö.; Foresman, J. B.; Ortiz, J. V.; Cioslowski, J.; Fox, D. J. *Gaussian 09, Revision C.1*; Gaussian, Inc., Wallingford, CT, 2009.
(29) Dupradeau, F.-Y.; Pigache, A.; Zaffran, T.; Savineau, C.; Lelong, R.; Grivel, N.; Lelong, D.; Rosanski, W.; Cieplak, P. *Phys. Chem. Chem. Phys.* **2010**, *12*, 7821−7839.
(30) Hornak, V.; Abel, R.; Okur, A.; Strockbine, B.; Roitberg, A.; Simmerling, C. *Proteins* **2006**, *65*, 712−725.
(31) Wang, J.; Wolf, R. M.; Caldwell, J. W.; Kollman, P. A.; Case, D. A. *J. Comput. Chem.* **2004**, *25*, 1157−1174.
(32) Pronk, S.; Pall, S.; Schulz, R.; Larsson, P.; Bjelkmar, P.; Apostolov, R.; Shirts, M. R.; Smith, J. C.; Kasson, P. M.; van der Spoel, D.; Hess, B.; Lindahl, E. *Bioinformatics* **2013**, *29*, 845−854.
(33) da Silva, A. W. S.; Vranken, W. F. *BMC Res. Notes* **2012**, *5*, 367−374.
(34) Hoover, W. G. *Phys. Rev.* **1985**, *A31*, 1695−1697.
(35) Parrinello, M.; Rehman, A. *J. Appl. Phys.* **1981**, *52*, 7182−7190.
(36) Daura, X.; Gademann, K.; Jaun, B.; Seebach, D.; Van Gunsteren, W. F.; Mark, A. E. *Angew. Chem., Int. Ed.* **1999**, *38*, 236−240.